Emissions Estimates for HC, CO, SOx and PM

For informational purposes, we have included the preliminary estimates of hydrocarbons (HC), carbon monoxide (CO), oxides of sulfur (SOx), and particulate matter (PM) emissions for the August 3-7, 1997 SCOS97 episode. The emissions for these pollutants were estimated for South Coast Air Basin waters (SCW) and for the SCOS97 domain.

For motorships, emission factors for cruising and maneuvering main engines and generators were obtained from Lloyd's Register Marine Exhaust Emissions Research Programme. For auxiliary boilers, emission factors in pounds per hour were used. (Acurex, December 12, 1996 and ARCADIS, May 28, 1999)

The steamship emission factors for HC, CO, PM, and SOx were obtained from the U.S. EPA AP 42 document. (U.S.EPA 1985) The gas turbines emission factors for these pollutants were obtained from JJMA. (Remley, 1998)

Tables B-3 summarize emissions for baseline (uncontrolled) HC, CO, PM, SOx for main engines, generators, and auxiliary boilers for the August 3-7, 1997 episode for the SCW.

Table B-3
Baseline HC, CO, PM, SOx Emissions for Main Engines, Generators (Auxiliary Engines), and Auxiliary Boilers for the August 3-7, 1997 Episode

Pollutant	Main Engines (Tons)	Generators (Tons)	Auxiliary Boiler (Tons)	Total (tons)
HC	2.3	1.0	0.5	3.8
CO	7.3	3.3	1.5	12.1
PM	6.7	2.9	1.6	11.2
SOx	65.2	24.5	61.5	151.2

The gridded emissions model was used to calculate ship emissions for the modeling region and for the South Coast waters. As shown in Tables B-4 and B-5, HC, CO, PM, and SOx emissions vary from day to day, due to differences in activity.

Table B-4
Gridded Ship Emission Totals (tons) for Each Day in August 3-7, 1997 Episode for Entire SCOS Modeling Region.

	Aug. 3	Aug. 4	Aug. 5	Aug. 6	Aug. 7	Total	Average per day
HC	1.9	2.1	1.1	1.4	1.8	8.2	1.6
CO	6.0	6.8	3.5	4.5	5.7	26.4	5.3
PM	5.3	5.9	3.1	4.2	5.2	23.7	4.7
SOx	58.2	59.8	35.3	51.5	63.5	268.2	53.6

Table B-5
Gridded Ship Emission Totals (tons) for Each Day in August 3-7, 1997 Episode for South Coast Waters Only.

	Aug. 3	Aug. 4	Aug. 5	Aug. 6	Aug. 7	Total	Average per day
HC	0.9	1.0	0.5	0.6	0.9	3.8	0.8
CO	2.7	3.2	1.7	2.0	2.5	12.1	2.4
PM	2.5	2.7	1.5	1.9	2.5	11.0	2.2
SOx	32.2	30.5	18.7	28.0	39.9	149.3	30.0

Table B-6
HC, CO, PM, and SOx Emissions for Ocean-Going Vessels for August 3-7, 1997 Episode (SCW and SCOS domain)*

HC	SCW					SCOS				
	8/3/97	8/4/97	8/5/97	8/6/97	8/7/97	8/3/97	8/4/97	8/5/97	8/6/97	8/7/97
BASE	0.86	0.96	0.49	0.63	0.86	1.86	2.05	1.06	1.40	1.84
S1	0.78	0.85	0.42	0.58	0.74	1.77	1.93	0.99	1.37	1.68
S2	0.67	0.73	0.37	0.49	0.60	1.65	1.80	0.95	1.30	1.49
S3	0.74	0.81	0.41	0.55	0.69	1.74	1.89	0.98	1.35	1.62
ALTP	0.88	0.98	0.50	0.64	0.88	1.99	2.20	1.13	1.51	1.97
CO	SCW					SCOS				
	8/3/97	8/4/97	8/5/97	8/6/97	8/7/97	8/3/97	8/4/97	8/5/97	8/6/97	8/7/97
BASE	2.75	3.21	1.66	1.95	2.52	5.99	6.76	3.51	4.48	5.69
S1	2.51	2.85	1.42	1.79	2.14	5.73	6.37	3.28	4.38	5.20
S2	2.14	2.48	1.26	1.51	1.70	5.33	5.94	3.17	4.15	4.58
S3	2.38	2.73	1.39	1.70	1.96	5.61	6.23	3.24	4.29	5.01
ALTP	2.81	3.27	1.69	1.99	2.59	6.44	7.24	3.75	4.84	6.12

*Baseline numbers may vary due to rounding.

Table B-6 (continued)
HC, CO, PM, and SOx Emissions for Ocean-Going Vessels for August 3-7, 1997 Episode (SCW and SCOS domain).

PM	SCW						SCOS				
	8/3/97	8/4/97	8/5/97	8/6/97	8/7/97		8/3/97	8/4/97	8/5/97	8/6/97	8/7/97
BASE	2.46	2.73	1.45	1.87	2.49		5.31	5.88	3.14	4.21	5.19
S1	2.25	2.41	1.24	1.72	2.15		5.06	5.53	2.94	4.12	4.75
S2	1.91	2.06	1.09	1.45	1.75		4.70	5.14	2.83	3.91	4.21
S3	2.14	2.30	1.22	1.64	2.00		4.97	5.40	2.91	4.05	4.59
ALTP	2.51	2.79	1.48	1.89	2.55		5.69	6.31	3.35	4.52	5.55
SOx	SCW						SCOS				
	8/3/97	8/4/97	8/5/97	8/6/97	8/7/97		8/3/97	8/4/97	8/5/97	8/6/97	8/7/97
BASE	32.22	30.47	18.72	28.03	39.89		58.17	59.82	35.28	51.51	63.46
S1	30.18	27.48	16.80	26.61	36.71		55.84	56.48	33.50	50.62	59.31
S2	27.14	24.18	15.34	24.02	33.17		52.46	52.79	32.42	48.47	54.51
S3	29.28	26.47	16.70	25.85	35.59		55.11	55.38	33.31	49.92	58.15
ALTP	32.72	30.96	18.94	28.26	40.41		61.59	63.93	37.05	54.30	66.53

* Base= Basecase, S1 = Scenario #1, S2 = Scenario #2, S3 = Scenario #3, S4 = Scenario #4, and ALTP = Proposed Shipping Lane

The U.S. Navy provided day-specific ship activity data for navy vessels traveling in the SCOS97 domain during the August episode. (See Table B-2) Table B-7 summarizes the emission estimates for the SCOS97 domain only.

Table B-7
Baseline HC, CO, PM, SOx Emissions* for U.S. Navy Vessels for August 3-7, 1997 Episode (SCOS domain).

HC (Tons)	CO (Tons)	PM (Tons)	SOx (Tons)
3	36	2	11

Due to time constraints, we have not been able to grid these emissions.

Estimate of Emission Reductions Attributable to the Precautionary Zone Speed Limit of 12 knots

To approximate the emission reductions that could be attributable to the 12 knot speed limit that was voluntarily instituted in 1994 we compared the expected emissions during the August episode under two assumptions: 1) assuming ships are abiding by the precautionary zone speed restriction of 12 knots; and 2) assuming the ships maintain cruise speed in the precautionary zone. As shown in Table B-8, the difference in emissions that can be attributed to the precautionary zone control (PZC) is approximately 5 tons during the episode or about a 6% reduction in cruising emissions. To estimate the impacts of the PZC on the 1997 SIP 2010 shipping emissions, we applied the control factor (0.06) to the projected 2010 cruise emissions for ocean-going ships adjusted for no PZC (27.8 T/D) in the 1997 SIP for the SCAB. This results in approximately a 1.7 T/D reduction that can be attributed to the PZC in 2010. This is a rough estimate as a more exhaustive analysis would need to consider the actual speeds that ships would travel in the precautionary zone without controls (i.e. ships may not be able to maintain cruise speed up to the breakwater) and differences in ship activity between 1997 and 2010.

Table B-8
Precautionary Zone Cruise (PZC) Air Quality Benefit
NOx Calculations for the August 3-7, 1997 Episode
(Ocean-going Cruise Emissions in the SCAB)

	Base Case*	No PZC Limit
	(Tons)	(Tons)
Cruise Main Engines	69.50	69.50
Cruise Generator	3.60	3.60
PZC Main Engines	11.40	5.70
PZC Generator	0.59	0.80
All Cruise Aux. Boiler	0.05	0.40
Episode Total	85.14	80.00

Ems Reduction for 5-Day Episode	NOx (tons)
	5.14

*Base Case = PZC without the 12-knot speed limit implemented
No PZC Limit = PZC with 12-knot speed limit not implemented, ships are assumed to travel at cruise speed in the precautionary zone

Appendix C

SCOS 97 Episode Classification

SCOS97 Episode Classification

An analysis was conducted to classify all days in 1997 including the SCOS97 episodes on the basis of the meteorological potential for ozone formation. The analysis utilized the Classification and Regression Tree Analysis (CART) ozone decision tree developed by Horie (1989) as a methodology for sorting and ranking each day into ten categories of ozone potential (terminal nodes). The Horie CART analysis classified the South Coast Air Basin daily maximum 1-hour average ozone concentration using daily surface wind characteristics and early morning upper air temperature profile in the coastal plain. Of the ten categories identified by CART, four categories (Episode Types I through IV) have been used to identify candidate meteorological episodes for regional modeling analyses conducted in support of the District's Air Quality Management Plan.

An air quality and meteorological database, consistent with that used by Horie's analysis, was constructed for each day in 1997. Using the CART tree as a map, each day was sorted based upon the observed daily meteorological profile. The results of the classification analysis are presented as a frequency distribution in Table C-1. Also presented in Table C-1 is the classification of the dependent data used by Horie for reference.

Table C-1
Classification of the 1997 Ozone-Meteorological Stagnation Potential

Horie CART Episode		1997 Distribution			Horie's Dependent Data (1982-1983)		
Ozone Potential	Met Class	Terminal Node	Number Count	Frequency Percent	Terminal Node	Number Count	Frequency Percent
Low		1	75	20.5	1	187	17.1
		2	35	9.6	2	199	18.2
		3	39	10.7	3	91	8.3
		4	18	4.9	4	113	10.3
Medium	Type IV	5	53	14.5	5	170	15.5
	Type III	6	81	22.2	6	86	7.8
		7	6	1.6	7	23	2.1
	Type II	8	25	6.8	8	124	11.3
	Type I-E	9	26	7.1	9	24	2.2
High	Type I	10	7	1.9	10	78	7.1

Analysis of the 1997 frequency distribution indicates that there were fewer low ozone potential days in 1997 than 1982-83 and roughly equivalent number of medium potential Type-IV ozone days for both periods. What is indicated in Table C-1 is that in 1997 there were fewer Type I and Type II episode days having higher potential for ozone and a greater number of Type III days where moderate levels of ozone were expected. Interestingly, in 1997 there was a reversal in the frequencies between terminal nodes nine and ten. Terminal node ten is a Type-I high potential ozone episode. Terminal node nine occurs under a similar meteorological profile as node ten however, a coastal eddy is typically developing and ozone potential is partially diminished under a lifting inversion.

Observations analyzed as part of the SCOS97 intensive monitoring forecasting program confirmed the frequency of eddy development during the summer months. The reduced ozone potential is indicative of the El Niño weather circulation that was building that summer.

Table C-2 lists the dates when the SCOS97 when intensive monitoring took place and the ozone-meteorological episode classification for each day listed. The majority of the days are classified as Horie episode categories I through III. The I-E eddy category is observed most frequently.

Table C-2
SCOS97 Intensive Monitoring Day Classification

Event Number	Date	Episode Node	Horie Category
1	8/4	9	I-E
2	8/5	9	I-E
3	8/6	9	I-E
4	8/7	10	I
5	8/22	9	I-E
6	8/23	9	I-E
7	9/3	6	III
8	9/4	10	I
9	9/5	6	III
10	9/6	8	II
11	9/22	6	III
12	9/23	9	I-E
13	9/27	6	III
14	9/28	8	II
15	9/29	6	III
16	10/3	5	IV
17	10/4	8	II
18	10/30	5	IV
19	10/31	6	III
20	11/1	9	I-E

Table C-3 lists the average resultant winds that were calculated for terminal nodes five through ten at seven District air monitoring stations located along the coast or in the coastal plain. The wind direction indicates where the wind vector originated. The net distance traveled through the wind monitoring station is also presented. What is evident from the calculation is that in 1997 the wind direction does not vary greatly by episode category. This is consistent even when the Type I-E eddy pattern is observed. Transport however is greatest for the Type I and Type II episodes (listed in terminal nodes 8 and 10). At the three stations closest to the coast (Hawthorne, Long Beach and Costa Mesa) transport for episode Type I-E is almost equal to the Type I episode.

The results of this episode classification indicate that the SCOS97 intensive field program captured meteorological episodes that were ranked in the top categories using the Horie model. Furthermore, while several of the episodes where characterized as Type I-E the wind analysis indicates that there was little difference in the net transport between a Type I and Type I-E episode at the coastal air monitoring stations.

Table C-3
1997 Average Resultant Wind Direction and Net Transport Miles for Terminal Nodes Five Through Ten
(Winds are from the direction listed. The 12-hour average includes hours 7 - 18.)

Station	Period	Variable	Pattern					
			5	6	7	8	9	10
West LA	24-Hr	Dir	217	222	214	222	212	216
	24-Hr	Miles	39	42	38	44	39	49
	12-Hr-	Dir	220	224	220	223	218	219
	12-Hr	Miles	38	37	37	41	39	46
Hawthorne	24-Hr	Dir	251	244	238	247	241	*243
	24-Hr	Miles	57	68	51	67	76	*107
	12-Hr-	Dir	251	244	238	246	246	*245
	12-Hr	Miles	45	54	47	52	58	*69
Central LA	24-Hr	Dir	244	240	235	246	242	235
	24-Hr	Miles	50	61	49	61	47	65
	12-Hr-	Dir	238	237	234	239	240	236
	12-Hr	Miles	45	48	40	49	47	57
Lynwood	24-Hr	Dir	210	213	205	217	221	218
	24-Hr	Miles	49	54	45	56	56	59
	12-Hr-	Dir	212	215	210	219	223	220
	12-Hr	Miles	38	41	35	44	44	47
Long Beach	24-Hr	Dir	201	204	192	217	231	223
	24-Hr	Miles	30	34	28	31	35	38
	12-Hr-	Dir	202	208	199	217	227	221
	12-Hr	Miles	26	28	25	26	29	32
Anaheim	24-Hr	Dir	203	212	192	217	231	223
	24-Hr	Miles	41	49	41	39	41	49
	12-Hr-	Dir	213	219	211	217	223	221
	12-Hr	Miles	31	36	31	30	32	39
Costa Mesa	24-Hr	Dir	238	238	212	237	243	234
	24-Hr	Miles	27	30	27	35	39	40
	12-Hr-	Dir	242	243	224	245	246	236
	12-Hr	Miles	25	26	24	30	33	36

* One Sample

References

Horie, Yuji, Ozone Episode Representativeness Study for the South Coast Air Basin , Appendix 5-P, 1989 Revision to the Air Quality Management Plan.

APPENDIX D

Summary of Comments and Responses

Summary of Written Comments and Responses

On April 14, 2000, the working draft of the TWG report,"Air Quality Impacts from NOx Emissions of Two Potential Marine Vessel Control Strategies in the South Coast Air Basin," was released for comment. Comment letters were received from the U. S. EPA, the Port of Long Beach, and the Steamship Association of Southern California. Below we provide a summary of written comments received and our responses.

Key:
- POLB — Port of Long Beach, May 10, 2000
- U.S. EPA — United States Environmental Protection Agency, May 5, 2000
- SASC — Steamship Association of Southern California, May 12,2000

1. Comment: *We believe there are errors in the calculations of transit time for the various vessels..... Until the transit times in each scenario have been checked and calculated if necessary, none of the scenarios appear valid. (*SASC)

Response: We have made the necessary corrections.

2. Comment: *Many of the new container vessels that have entered the trade in the past twelve to eighteen months and that are entering today have new larger engines that will have a variety of impacts on any proposed rule. For example, we have learned the engines in the ships of a large Danish owner must use an auxiliary diesel to assist the engine's turbo charger when the vessel's speed reaches 18 knots or less. Thus, we may loose some NOx benefits by reducing this vessel's speed to 15 knots or 12 knots.* (SASC)

Response: Estimating the effect of this information on the emission reduction estimates for the speed reduction strategy is not straightforward and is probably best addressed in conjunction with a revision to the baseline inventory. Regardless, the results of the comparative analysis are not dependent on future projections of emissions and this new data does not modify the conclusions in the report.

3. Comment: *The vessel used in the base case, the M/V "Tundra King" has only called at LA/LB once in the past five years, thus it is not representative of vessels that call at the San Pedro Bay ports.* (SASC)

Response: In the analysis of the impact of shipping emissions, we looked at the aggregate ship emissions during the episode. The analysis was not designed to evaluate the emissions from individual ships. In the aggregate, the numbers and proportions of ship types traveling the shipping lanes during the August episode are consistent with data available for 1997 (See Table D-1). While we acknowledge there are some differences, we believe that the data available demonstrates that there are not substantial differences between the episode ship types/numbers and those for other years. Based on this comparison, we believe the data is representative of the ships using the San Pedro Ports.

Table D-1
Ship Calls by Ship Type

Ship Type	Ocean Going Vessels Calling on the Ports of Los Angeles and Long Beach as a Percent of Ship Type for the Time Period Identified	
	August 97 Episode	1997*
Auto	6.9%	5.02%
Bulk Carrier	13.7%	16.4%
Container Ship	54%	44.8%
General Cargo	3.4%	4.6%
Passenger	3.4%	6.1%
Reefer	3.4%	5.2%
Roll-on/Roll-off (RORO)	1.1%	1.2%
Tanker	13.7%	14.1%
Average Number Ships per Day	17	14

* Data taken from "Marine Vessels Emissions Inventory Update to 1996 Report: Marine Vessel Emissions Inventory and Control Strategies,"Arcadis Geraghty & Miller, 23 September 1999 prepared for the South Coast Air Quality Management District.

4. Comment: Page 1, *Executive Summary. The first bullet near the bottom of the page ("the voluntary ...") is a bit wordy. Can it be rewritten so that its meaning is more easily understood?* (U.S. EPA

Response: The first bullet was rewritten as requested.

5. Comment: *Page 3, Public Consultative Process. It's probably not necessary to mention the three workgroups since this report focuses only on Deep See Vessel/Shipping Channel issues.* (U.S. EPA)

Response: The section was modified as suggested.

6. Comment: *Page 4, 2nd paragraph. Last sentence should be past tense (i.e., "Participation was open ..."). page 4, last paragraph, 1st sentence. Same comment as above.* (U.S. EPA)

Response: We included the suggested revision into the report.

7. Comment: *Page 5, last sentence. The last portion of the sentence should be reworded. "... that may need to be considered ~~evaluated~~ when a decision is made regarding the most appropriate operational control for marine vessels. ~~U.S. EPA undertakes a formal rulemaking~~* (U.S. EPA)

Response: We included the suggested revision into the report.

8. Comment: *Page 7, Table II-1. Please provide references for the information, especially for average MAREX and average design speed.* (U.S. EPA

Response: We added references to Table 11-1 as requested.

9. Comment: *Page 10, last sentence in partial paragraph at the top of the page (and elsewhere in the report). The mention of photochemical analysis needs to be clarified. The need for photochemical analysis is stressed elsewhere (most notably on p12 and in the conclusions), but there is no real discussion of why photochemical modeling is needed. What additional information would it provide? If the options were modeled using photochemical analysis, could it possibly change the conclusions? If so, how? The report also implies that photochemical modeling will be done later. This could be interpreted as all of the options will be modeled, but from the last meeting, our understanding is that only the preferred option will be modeled. We are not suggesting that mentioning the need for photochemical modeling should be deleted from the report, we are recommending that the issue be further explained. (U.S. EPA*

Response: We provided further explanation in the discussion on photochemical modeling included in Appendix A, "Scope of Analysis."

10. Comment: *Pages 11 and 12, Scope of Analysis. As discussed at the last meeting, it may make sense to move these issues to an appendix. You could state in the report that because of time and resource considerations, the report did not address the issues listed in Appendix ( ). Also, we recommend that the reference to future actions should be rewritten as: ~~will need to be addressed by U.S. EPA when a rulemaking is undertaken.~~ may need to be considered when determining the most appropriate operational control for marine vessels. (*U.S. EPA)

Response: We added a new Appendix A which describes the "Scope of Analysis." Any reference to future U.S. EPA actions were rewritten as suggested.

11. Comment: *Page 12. For the issues that may need additional analysis (e.g., Impacts beyond SCAB Boundaries; Economic, Logistic and other impacts), can wording be added stating that EPA intends to continue to work with members of the TWG to assist in resolving the issues?* (U.S. EPA)

Response: We included wording as suggested by U.S. EPA.

12. Comment: *Page 76. 1st paragraph. Please delete ⊙to fulfill their obligations in the 1994 Ozone SIP.○ EPA has never agreed that they were obligated to fulfill the reduction targets in the 1994 SIP. Also, please rewrite the last sentence. It would be much cleaner to say that the TWG agreed to limit its analysis to the SCAQMD and that impacts to upwind*

and downwind areas may need to be considered when determining the most appropriate operational control for marine vessels. (U.S. EPA)

Response: The reference in the first paragraph to U.S. EPA's role in the SIP was reworded to be consistent with the language in the January 8, 1997 Federal Register notice approving the California SIP. The last sentence was reworded to improve the readability.

13. Comment: *Page 79, Table VI-4. There needs to be some explanation, methodology, and a spreadsheet that shows how to reductions were calculated. (This could be placed in an appendix.) The footnote below the table indicates that the control factors were multiplied times the projected 2010 NOX emissions (26.2 tpd). Please clarify what emission sources make up the 26.2 tpd estimate. Is this only cruise emissions or does it include maneuvering and hoteling? How does the 26.2 estimate account for current reduced speed in the precautionary zone?* (U.S. EPA)

Response: We modified this section to better describe the methodology used for estimating potential SIP credits from the various control strategies.

14. Comment: *The purpose of the Windfield Validation analysis is to determine whether the results of the tracer study are sufficiently well represented by the model simulations, that there is a reasonable expectation that model results for other simulated periods can be accepted as meaningful. In fact, the attempts to replicate the tracer results by means of modeling were inconclusive at best. In general, the calculated onshore fluxes were much lower for the tracer measurements than in the model simulations, and only 2-10 percent of the tracer mass released was accounted for by the measurements. The one possible explanation for this discrepancy that is never raised in the report is that less of the real tracer may have actually come onshore than the model predicted. It is encouraging that the modeling was able to conserve tracer mass during the simulations, but that does not mean the model was replicating reality. The fact that most of the real tracer mass apparently was not detected at the monitors onshore is masked in Figures V9-V13, by the practice of normalizing the results for each tracer (dividing each calculated percentage flux by the highest calculated value). When this is done the apparent percentages of tracer mass coming on shore in different areas more closely match the magnitude of values predicted by the model, but it is not clear whether this actually reflects better model performance. Calculation of correlation coefficients for the various comparisons that are presented between model-predicted and measured parameters would help to clarify this issue.* (POLB)

Response: The objective of the Model Validation portion of the analysis was to demonstrate that the simulated results were consistent with those observed from the tracer experiment. In the analysis, this consistency was illustrated by comparing the *relative* mass distributions from the simulation results to that estimated from the observations. This analysis was limited by the fact that there is no straightforward way to accurately estimate mass flux from observational data for reasons listed in the report. Among these reasons are lack of knowledge of the vertical distributions of the tracer concentrations and limited knowledge of the horizontal distribution based on the spatial resolution of the sampling network relative to

the scale of the tracer plumes. We agree that the conclusions from the analysis must be interpreted in this light.

However, we believe that the observational data from the experiments suggest that the tracer material came onshore in relatively narrow plumes. In many cases, the plumes were so narrow that the various tracers were only detected at one or two sampling points along the coastline. We acknowledge the limited sampling network in Ventura and San Diego Counties, however peak tracer concentrations were recorded well within the limits of the sampling network. These observations are consistent with the assumption that most of the tracer mass came onshore within the limits of the sampling network.

We acknowledge that only 2-10 percent of the tracer mass was accounted for in the calculations based on the observed tracer concentrations. Those numbers could easily have been increased by reviewing the assumptions made about the horizontal and spatial distributions of the tracers on an hour-by-hour basis. However, any such assumptions would not change the *relative* mass distribution. The comparisons between the simulated and observed mass fluxes were based on *relative* concentration distributions. Thus, even if different assumptions were made to increase the observed mass, the simulated relative mass distribution that did come onshore would remain consistent with that calculated from the observations.

15. Comment: *The wind fields were peer reviewed for the period August 3-7, but not for September 4-5. Day-specific emissions data were available for the August period, but not for the September period (which was modeled with August emissions). It would appear that more confidence should be placed in the results of the August 3-7 model simulations, for which the proposed shipping lane scenario was predicted to produce the largest or second largest emission reductions on four of the five days and was less effective than speed reductions only on a day for which the predicted concentrations were very low. Although the simulations for September 4-5 are flawed by the attempt to superimpose emissions and meteorology from different periods, those results also indicated more beneficial impacts for the proposed shipping lane on two of the three days. It is therefore quite surprising that the study concludes from these results that the speed reduction control approach is preferable to the proposed shipping lane approach.* (POLB)

Response: Although peer review of the September episode was not completed, some peer review of that episode did occur (as well as the windfield validation). Areas of concern for that episode were investigated with a sensitivity simulation; this simulation suggested that the modeling results were not sensitive to the identified concerns.

The TWG agreed that the August 3-7 emissions were typical enough to be used for the September episode. It is worth noting, however, that there is no physical link between the pattern of offshore emissions on any given day and the meteorological patterns. In effect, the offshore emissions and the meteorological flow patterns for each day represent random samples wherein, from a probability standpoint, any combination of offshore emissions and meteorology can occur on any given day. In the report, this issue was addressed in the discussion of variations in daily emissions (see pages 71-73).

The conclusions of the report are based on analysis results showing that the relative impact of the alternative shipping lane can vary widely from one day to the next, and may even result in a significant disbenefit on some days, while the relative impacts from the speed-control scenarios are consistently beneficial. This finding was consistent between the tracer analysis and modeling results.

16. Comment: *The data presented for the route of the tracer release on the September afternoon offshore proposed shipping alternative test (Figure IV-3) shows that 40 percent of the tracer emissions being released were within 25 miles of the shore, as compared no tracer emissions being released within this region for the August afternoon proposed alternative channel route test (Figure IV-2). Due to the variations in the locations, results would be expected to vary significantly, as seen in the results. It would seem that the August event is more representative of the proposed shipping channel alignment. This, combined with the validated data for August time period and the actual ship inventory, indicate that the August data provides a better set of comparisons for review.* (POLB)

Response: As discussed in Chapter V, actual shipping emissions were simulated along the ship paths. For the early September episode, the August emissions were used as per the TWG. However, any combination of offshore emissions and meteorology can occur on any given day. We believe that the consistency in findings between the tracer and simulation analyses adds to the credibility of the results for both episodes.

17. Comment: *The conclusions on page 43 that the proposed shipping channel resulted in increased impacts on San Diego are based upon only three observations during three of the tests. Furthermore, one of the observations was orders of magnitude below the other averaged values (Table IV-12). Accordingly, those conclusions should be removed from the report* (POLB)

Response: We agree that the conclusions regarding San Diego are based upon very limited data (one monitoring site), and have removed those conclusions from the report.

18. Comment: *The meteorological interpolation used in CALMET employed interpolation barriers to limit offshore extrapolation from onshore wind monitoring sites. However, on page 45, Figure V-2, there is no offshore/onshore barrier used to restrict onshore influences to offshore wind flow as it enters the SCAB, as done near the Ventura County shoreline. Since there were very few sites offshore and no barriers, the modeling would allow a stronger influence of onshore monitors when calculating offshore wind flow patterns, thus biasing the meteorological wind field for subsequent analyses.* (POLB)

Response: The interpolation barrier used with CALMET offshore of Ventura and Los Angeles Counties is based on the understanding that NNW winds offshore are stronger along this portion of the coastline than they are further south (which is partly protected by the Palos Verdes peninsula). This understanding is supported by the results of the September tracer experiment which showed tracer material released near Anacapa Island

coming onshore in Orange County. However, it is not considered unique to the September episode period.

19. Comment: *In the CALGRID modeling for the morning existing channel - PDCH (page 48) and the morning proposed channel - PTCH (page 49) it is unclear why the overland mass increases as soon as the release is made. It would appear that the mass would need travel time over water reaching the shore, as seen in the PMCH, PMCP, and PDCB analyses (pages 48-50).* (POLB)

Response: The observed feature is an artifact of Eulerian models. It can be characterized as the result of numerical or "artificial" diffusion. While ships are acknowledged point source, the minimum spatial resolution of the model is 5 km. Thus, after the first incremental time step (about 8 minutes), any emissions fill a three-dimensional 5x5x5 km grid cell. During the second time step, some of the mass is diffused into adjacent grid cells. Model output occurs after 60 minutes, or approximately 8 time steps. Thus, diffusion in an Eulerian model is typically greater than in the real world.

20. Comment: *The report appears to rationalize poor relationships between observed and predicted results on page 54, first paragraph (and page 60). It is true that a plume produced by a stationary point source may not hit a specific receptor location. However, the ships are not a stationary point source, but are more accurately represented as a line source over time. Accordingly, the argument presented is not valid.* (POLB)

Response: We acknowledge that a single moving ship is a moving point source. However, that does not invalidate the point being made. In an ideal case, the emission source would be moving parallel to the coastline with winds perpendicular to the coastline. In such a case, the plume would be detected all along the coast and would be easy to characterize. Unfortunately, during the tracer experiments the tracers released offshore where detected onshore at only a few sites, suggesting relatively narrow plumes relative to the spatial density of the sampling network. In such instances, the chances of being able to determine the peak concentration within the plume were limited.

21. Comment: *The first five sections of the report allow a reader to draw one of two conclusions: (1) the study is inadequate as a basis for selecting among the control alternatives; or (2) the proposed shipping lane may reduce onshore impacts on more days than the speed reduction measures, including more days when the potential for significant onshore advection of shipping emissions is highest. Section VI alters these results by adjusting their significance according to their likelihood of occurrence. This is accomplished by the application of some weighting factors that purport to incorporate consideration of the relative frequencies of the conditions under which different results were obtained. There is a reference to an analysis of ozone episode categories in Appendix B, but the manner in which these weighting factors are derived from that analysis is not explained either in Section VI or in Appendix B. The reader is asked to take this final adjustment of the study results on faith, and to accept that this is the justification for showing a more favorable result for the speed scenarios. The technical basis for this weighting procedure, which reverses the results that would otherwise have to be reported, must be made clear.* (POLB)

Response: We believe that the most obvious conclusion from the report is that the relative impact of the alternative shipping lane can vary widely from one day to the next, and may even result in a significant disbenefit on some days, while the relative impacts from the speed-control scenarios are consistently beneficial. This finding was consistent between both the tracer analysis and modeling results. Of the types of days analyzed and simulated, it is certainly true that there is a dispersion benefit for more types of days for the alternate shipping lane. However, the analysis of frequency of occurrence of the different days in 1997 showed that the type of day for which there was a disbenefit to the alternate shipping lane was more prevalent than the other types of days.

We acknowledge that the presentation of and discussion about the use of the frequency distributions needs to be expanded and clarified and have revised the discussion as recommended.

22. Comment: *One of the primary reasons for advocating of the alternate shipping lane has been the premise that emissions released further offshore will generally reach onshore areas of the SCAB less often than emissions closer to shore. This issue is not addressed by this study, which only analyzed/modeled days when some onshore flow was known to occur. In fact meteorological frequency issues are not brought into the analysis at all until the final presentation of the findings, and as noted previously, the technical basis for these final adjustments is not explained.* (POLB)

Response: As indicated above, we agree that the discussion about the use of the frequency distributions needs to be clarified and have revised this section to provide more explanation. We appreciate the comment that the analyses conducted for this study did not address all types of offshore flow days. That task was beyond the limited scope of this study, and would require a great deal of resources and data that are not currently available.

23. Comment: *We agree that photochemical modeling that includes the contributions of all NO_x and VOC sources within the air basin is needed to assess the relative benefits/disbenefits of the alternate control measures. In fact, modeling of NO_x as an inert pollutant and relying on the calculations of relative dispersion of shipping emissions as a basis for evaluating NO_x control options could lead to misleading results. Depending on the VOC/NO_x ratios in specific areas, higher NO_x concentrations moving onshore could act either to increase or to decrease local ozone levels.* (POLB)

Response: From a technical standpoint, we would agree that photochemical modeling could potentially provide additional information on the fate of shipping NO_x emissions in the context of the overall inventory, assuming satisfactory model performance. However, the decision to not include photochemistry in this analysis was made by the TWG early in the process, based on the unavailability of a complete emissions inventory and due to the preliminary standing of the SCOS meteorological inputs. Please see the response to Comment #9.

24. Comment: *Based upon Item 3 above, it would appear that the report incorrectly states (in the last paragraph on Page 9) that the onshore emission impacts were compared with the results from tracer tests to perform a comparative analysis. Since a majority of the comparisons were performed on the September event and the September data was not validated, these comparisons are suspect.* (POLB)

Response: We modified the last paragraph to improve the clarity. With regards to using the September episode, as stated previously in the response to Comment #15, the TWG agreed the August 3-7 emission were representative of typical shipping emissions and could be used for the September episode.

25. Comment: *On Page 14, first line, it should state, "...emission rates for auxiliary boilers and diesel engines were obtained from Lloyds....".*(POLB)

Response: The correction has been made.

26. Comment: *The last sentence on Page 20 is inaccurate. In general, steamships do not have auxiliary boilers.* (POLB)

Response: This paragraph has been revised.

27. Comment: *Table III-8 on Page 22 does not appear to represent appropriate transit times for the cases. Although there is a change to the entry column for Scenario #2, other columns appear questionable. The exit times for Base Case and Scenario #3 are the same, even though there is a 15 mph speed restriction on the ships out to the SCAB overwater boundary. Also, entry times for the Base Case are greater than Scenario #1 for all ships, with a 12 mph restriction from 20 miles out. Entry times are identical for Base Case and Scenario #3 for most of the ships.* (POLB)

Response: Table III-8 has been revised.

28. Comment: *Figure II-2 on Page 9 should actually be credited to "control of Ship Emissions in the South Coast Air Basin", August 1994, prepared by the Port of Los Angeles and the Port of Long Beach.* (POLB)

Response: We agree there was an error and have made the suggested revision.

California Environmental Protection Agency
AIR RESOURCES BOARD

STAFF REPORT: INITIAL STATEMENT OF REASONS FOR PROPOSED RULEMAKING

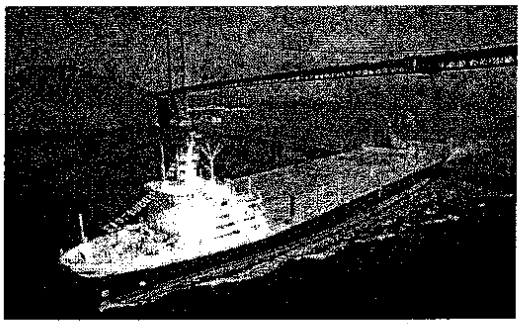

PROPOSED REGULATION FOR AUXILIARY DIESEL ENGINES AND DIESEL-ELECTRIC ENGINES OPERATED ON OCEAN-GOING VESSELS WITHIN CALIFORNIA WATERS AND 24 NAUTICAL MILES OF THE CALIFORNIA BASELINE

Stationary Source Division
Emissions Assessment Branch
October 2005

Appendix F

Offshore Emissions Impacts on Onshore Air Quality

OFFSHORE EMISSIONS IMPACTS ON ONSHORE AIR QUALITY

The transport of air pollution over long distances and between air basins is well established. The emissions from ocean-going vessels (OCVs or vessels) can travel great distances and numerous studies have shown local, regional, and global impacts on air quality. (Endresen, 2003; Jonson, 2000; Corbett and Fishbeck, 1997; Streets, D.G., 2000; Saxe, H. and Larsen, T., 2004) Ocean-going vessels emit large quantities of several pollutants, however, the impacts of nitrogen oxides (NOx) and sulfur oxides (SOx) are the most often studied using various air quality models. In a recent study, using a bottom-up estimate of fuel consumption and vessel activity for internationally registered fleets, annual emissions from vessels worldwide were estimated to be significantly greater that previously considered. This study estimated that the global NOx from vessels is actually more than doubled from previous estimates. This study also suggests that near shore emissions impacts may be much larger than previously estimated. (Corbett and Koehler, 2003) Other studies indicate that vessel emissions can be a dominant contributor to sulfur dioxide concentrations over much of the oceans and in many coastal regions. (Capaldo, 1999) However, NOx and SOx are not the only pollutants of concern, as additional studies show coastal ozone and particulate matter impacts from OCV emissions. (Marmer and Langmann, 2005; Lawerence and Crutzen, 1999; Fagerli and Tarrasson, 2001; Eastern Research Group and Starcrest Consulting Group, 2003)

A study for the International Maritime Organization concludes that at any given time, most vessels are near a shore and that approximately 80 percent of the emissions are emitted near the coast, including the west coast of the United States. (International Maritime Organization, 2000) In California, ship emissions are becoming an increasingly important source of emissions as their relative contributions to the total amount of pollution is increasing as land based sources become more stringently controlled. For example, the Santa Barbara County Air Pollution Control District estimates that by 2015, NOx emissions from ships will comprise more than 60 percent of their total NOx inventory. (Murphy)

The issue of onshore impacts of offshore emissions has been a concern in California for several decades. Tracer studies, analysis of meteorological data and ambient monitoring data, and air quality modeling, are approaches used to determine the extent to which emissions released offshore can impact onshore areas.

Tracer Studies

Tracer studies have been conducted off the California coast to determine characteristics of pollutant transport in California's coastal areas and they provide evidence of onshore impacts from offshore emissions. A tracer study involves the release of a known amount of a non-toxic, inert gas from either a moving or

fixed point offshore and the subsequent sampling the of the atmosphere for concentrations of that gas at sites onshore. Brief descriptions of three such studies, from which we can infer that pollutants emitted from offshore ships can be transported to onshore areas and be available to participate in onshore atmospheric processes, are given below.

In 1977, a dual tracer study was conducted from a naval research vessel traveling 8 to 20 miles offshore. (ARB, 1983) The two tracers, sulfur hexafluoride and bromotrifluromethane were released as the ship moved from the Long Beach area to the Santa Barbara channel. Twenty-nine onshore sites were established to monitor for the two tracers. The results showed both tracer gases were detected at sampling stations along the entire length of the network that ran from Ventura to Long Beach.

Another tracer study involving the Santa Barbara Channel conducted in 1980 was performed to collect data to be used in an air quality model and again showed pollutants emitted offshore were detected onshore. (ARB 1982; ARB 1984) This study used sulfur hexafluoride in six tracer experiments emitted offshore and at Point Conception. Over 10,000 samples were gathered from on-shore sites and also from boats and airplanes to determine offshore transport paths. The results showed that pollutants emitted in the Santa Barbara Channel will be transported onshore and that very little dispersion occurs over water, and as a consequence, the pollutant concentration downwind can be elevated.

The most recent of the tracer studies discussed here was conducted as part of the 1997 Southern California Ozone Study. (ARB, 2000) The objectives of this tracer study were two-fold. The primary objective was to obtain direct evidence regarding the trajectory of emissions from vessels transiting the coast and the impact on onshore air quality from two proposed shipping lanes. The secondary objective was to assess the ability of models to simulate the relevant physical processes that take place during transport of emissions offshore from the shipping lanes to onshore. A total of 51 onshore sampling site locations were selected from Santa Barbara to Oceanside, going inland as far as Santa Clarita Valley and the Rubidoux air monitoring station. Five perfluorocarbon (PFTs) tracers were used in this study. The tracer gases were released from both a fixed point offshore and from vessels moving simultaneously along two shipping lanes for a specified period of time. The results of the study showed that the tracer gases were detected on-shore and suggested that meteorology strongly influences the direction and magnitude of dispersion of the pollutants.

Meteorology/Climatology

Another source of information regarding onshore impacts is to examine the meteorology/climatology near the coast. In the early 1980's, based on a investigation of meteorological data, the Air Resources Board established the California Coastal Waters (CCW) as a boundary within which emissions that are

released, are transported on-shore. In addition, ARB meteorology staff recently reviewed available data to determine if California meteorological and climatology support the transport of offshore emissions to coastal air basins. A brief discussion on the development of the CCW and the more recent data review is presented below.

California Coastal Water Boundary: Previous studies by the ARB have demonstrated that pollutants released off California's coast can be transported to inland areas due to the meteorological conditions off the coast. In 1983, in the Report to the Legislature on Air Pollutant Emissions from Marine Vessels, the ARB established a boundary based on coastal meteorology within which pollutants released offshore would be transported onshore (ARB, 1983; ARB, 1984). The development of the boundary defined as the California Coastal Waters (CCW) is based on over 500,000 island, shipboard, and coastal observations from a variety of records, including those from the U.S. Weather Bureau, Coast Guard, Navy, Air Force, Marine Corps, and Army Air Force. (ARB, 1984) The area within the CCW boundary is defined as that area between the California coastline and a line starting at the California Oregon border at the Pacific Ocean. The California Coastal Waters are shown in Figure 2. This boundary ranges from about 25 miles off the coast at the narrowest to just over 100 miles at the widest.

Figure 2: California Coastal Waters

"California Coastal Waters" means that area between the California Coastline and a line starting at the California-Oregon border at the Pacific Ocean

thence to 42.0°N 125.5°W
thence to 41.0°N 125.5°W
thence to 40.0°N 125.5°W
thence to 39.0°N 125.0°W
thence to 38.0°N 124.5°W
thence to 37.0°N 123.5°W
thence to 36.0°N 122.5°W
thence to 35.0°N 121.5°W
thence to 34.0°N 120.5°W
thence to 33.0°N 119.5°W
thence to 32.5°N 118.5°W

and ending at the California-Mexico border at the Pacific Ocean. Coordinates shown above are exact. Distances of California Coastal Waters boundary from coast are rough

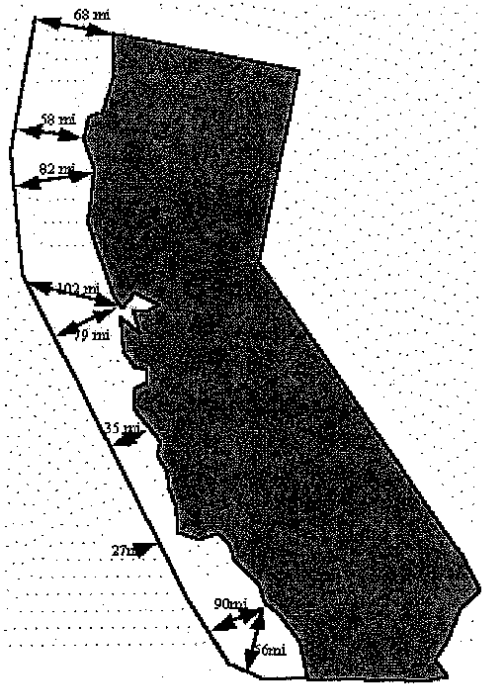

approximations.

Review of Available Meteorological and Climatological Data: As previously documented in reports by the ARB (ARB, 1983; ARB 1984) the lower atmosphere is the medium in which air pollution is carried from one surface or near-surface pollution source to a surface based receptor. In this medium, the direction of pollution transport and the dispersion of air pollutants are largely dependent upon the wind and the vertical temperature distributions (stability).

The wind and the stability along the coast of California are largely affected by the North Pacific high pressure cell, particularly during the summer. It is a semi-permanent feature of the Northern Hemispheric large scale atmospheric circulation pattern, and it produces a predominantly northwesterly flow of maritime air over the California coastal waters. This circulation pattern is modified to more westerly flow by continental influences as the air approaches the coast of California.

Another California weather characteristic that results from the location of the Pacific high is the steady flow of air from the northwest during the summer that helps drive the California Current of the Pacific Ocean. The California Current sweeps southward almost parallel to the California coastline. However, since the mean drift is slightly offshore, there is a band of upwelling immediately off the coast as water from deeper layers is drawn into the surface circulation. The water from below the surface is colder than the semi-permanent band of cold water just offshore, which ranges from 25 to 50 miles in width.

The temperature of water reaching the surface from deeper levels is as much as 10° colder during the summer than is the water 200-300 miles farther west. Comparatively warm, moist Pacific air masses drifting over this band of cold water form a bank of fog which is often swept inland by the prevailing northwest winds out of the high pressure center. In general, heat is added to the air as it moves inland during these summer months, and the fog quickly lifts to form a deck of low clouds that extend inland only a short distance before evaporating completely. Characteristically, this deck of clouds extends inland further during the night and then recedes to the vicinity of the coast during the day. This layer of maritime air is usually from 1,000 to 2,000 feet deep, while above this layer the air is relatively warm, dry, and cloudless.

Additionally, the air flowing around the Pacific high at upper levels is sinking (subsiding) and consequently warming due to compression. This warm air above the cool coastal marine air produces a strong, persistent vertical temperature inversion which limits the vertical mixing of pollutants.

As stated above, the North Pacific high pressure cell produces a predominantly northwesterly flow of marine air over California Coastal Waters and, generally, this flow becomes more westerly as the air approaches the coast of California.

Numerous climatological studies which describe the air flow patterns along the California coast clearly show this. Table 1 presents a summary of the wind flow direction frequencies measured at various locations along the California coast as shown in previous ARB reports. The table shows that onshore wind flow predominates during the spring and summer at all five locations, and during the fall at four out of the five sites. The table also shows that, on an annual basis, onshore winds are about twice as common as offshore winds at those given locations. The data in Table 1 are based on a relatively large data set. Because the data set covers multiple years, these wind flow percentages are not expected to change significantly over time. However, data from a more recent analysis are provided in Table 2 to show the consistency in wind flow patterns through the years. Table 2 shows the predominant wind flow at various coastal sites in California. The directions that are shaded correspond to onshore conditions. All coastal sites depicted in this table are dominated by onshore conditions and each site has at least eight months where onshore flow is the dominant wind direction. The data in Table 2, although depicted slightly different, are consistent with the data in Table 1.

Table 1: Wind Flow Direction Frequencies in Coastal Areas of California[1]

Station	Wind Direction	Seasonal Frequency[2] (%)				
		Spring	Summer	Fall	Winter	Annual
Oakland	Onshore	75	83	62	47	67
	Offshore	20	13	27	42	25
	Calm	5	4	11	11	8
Vandenberg AFB	Onshore	64	69	48	34	54
	Offshore	24	9	32	53	29
	Calm	12	22	20	13	17
Santa Barbara	Onshore	50	62	44	32	47
	Offshore	26	21	29	24	25
	Calm	24	17	27	44	28
Point Mugu NAS	Onshore	57	59	41	31	47
	Offshore	28	21	41	54	36
	Calm	15	20	18	15	17
Los Angeles	Onshore	68	81	60	43	63
	Offshore	30	16	36	53	34
	Calm	2	3	4	4	3

Source: National Climatic Center
1.Period of Record:
Oakland – 1965-1978
Vandenberg AFB – 1959-1977
Santa Barbara – 1960-1964
Point Mugu NAS – 1960-1972
Los Angeles International – 1960-1978

2. Spring: March, April, May;
Summer: June, July, August;
Fall: September, October, November; and
Winter: December, January, February

Table 2: Prevailing Wind Direction at California Coastal Sites[1] (1992-2002)

Station[2]	JAN	FEB	MAR	APR	MAY	JUN	JUL	AUG	SEP	OCT	NOV	DEC
SFO	WNW	WNW	WNW	WNW	WNW	WNW	WNW	WNW	WNW	WNW	WNW	WNW
MRY	ESE	ESE	WNW	WNW	WNW	WNW	WNW	WNW	WNW	WNW	ESE	ESE
SBA	WSW	WSW	WSW	WSW	WSW	WSW	WSW	WSW	WSW	WSW	WSW	WSW
OXR	WNW	WNW	WNW	WNW	WNW	WNW	WNW	WNW	WNW	WNW	WNW	NE
NTD	NE	WNW	WNW	WNW	WNW	WNW	WNW	WNW	WNW	WNW	NE	NE
SMO	SSW	SSW	SSW	WSW	SSW	SSW	SSW	SSW	SSW	SSW	SSW	N
LAX	E	WSW	WSW	WSW	WSW	WSW	WSW	WSW	WSW	WSW	WSW	E
SNA	SSW	SSW	SSW	SSW	SSW	SSW	SSW	SSW	SSW	SSW	SSW	SSW
OKB	WNW	NE	WSW	WSW	WSW	WSW	WSW	WSW	WSW	WSW	WSW	NNE
SAN	WNW	WNW	WNW	WNW	WNW	WNW	WNW	WNW	WNW	WNW	WNW	WNW

Source: Western Region Climate Center (http://www.wrcc.dri.edu/)

[1] Prevailing wind direction is based on the hourly data from 1992-2002 and is defined as the direction with the highest percent of frequency. Wind directions that are shaded correspond to onshore flow.

[2] SFO – San Francisco International Airport; MRY – Monterey Airport; SBA – Santa Barbara Airport; OXR – Oxnard Airport; NTD – Point Mugu Naval Air Station; SMO – Santa Monica Airport; LAX – Los Angeles International Airport; SNA – Santa Ana Airport; OKB – Oceanside Municipal Airport; SAN – San Diego Lindbergh Field

As stated above, the large scale climatological wind flow along the California coast is modified by the effects of local land/sea breeze circulations. In effect, the local daytime sea breeze enhances the large-scale onshore component of the wind while the nighttime land breeze retards or occasionally reverses the flow. Table 3 presents seasonal resultant winds by time of day for San Francisco International Airport and Point Mugu Naval Air Station. The table shows the influences of the land/sea breeze circulations and shows that the onshore winds are generally stronger than offshore winds, a further indication of the transport of offshore emissions to receptor areas onshore.

Table 3: Seasonal Resultant Winds
(Degrees/MPH – Onshore Winds Shaded)

	San Francisco (International Airport)					Point Mugu NAS				
Time (PST)	Spring	Summer	Fall	Winter	Annual	Spring	Summer	Fall	Winter	Annual
0100	323/2	287/3	281/2	252/1	280/2	323/1	Calm	036/2	033/4	024/1
0400	272/1	284/3	276/2	224/1	276/2	007/1	029/1	032/2	036/4	030/2
0700	274/1	282/6	270/2	180/1.4	277/2	013/2	013/1	031/2	038/4	029/2
1000	305/1	306/22	350/2.0	084/2.1	320/2	330/4	235/5	216/1	052/4	230/2
1300	292/10	297/16	307/6	015/1.7	299/8	250/8	282/8	219/5	280/2	249/6
1600	281/2	289/17	290/10	299/8	288/7	261/9	267/8	269/6	279/3	268/7
1900	250/1	289/10	289/8	282/4.0	286/5	270/6	267/4	320/2	001/2	297/3
2200	280/9	289/11	287/8	266/2.3	284/7	297/2	291/1	002/2	022/3	340/2
All Hours	281/3	291/13	291/8	276/1.3	287/6	269/3	264/3	300/1	022/2	288/2

In addition, the ARB staff categorizes air flow for the four most heavily populated air basins in California: Sacramento Valley, San Joaquin Valley, San Francisco Bay Area, and the South Coast Air Basin three times a day. See Figure 1 for an example of the air flow types relevant to the San Francisco Bay Area and South Coast Air Basins.

Onshore and offshore percentages can be obtained by grouping the types appropriately. For instance, air flow types Ia, Ib, II, V, and VI would correspond to onshore conditions in the San Francisco Bay Area. Air flow types I, II, and IV would reflect onshore conditions in the South Coast Air Basin. The results are illustrated in Table 4. The onshore/offshore prevalence for these air basins based on this kind of air flow typing is consistent with the onshore/offshore frequencies of individual sites in these areas shown from prior analyses.

Figure 1

San Francisco Bay Area Air Basin

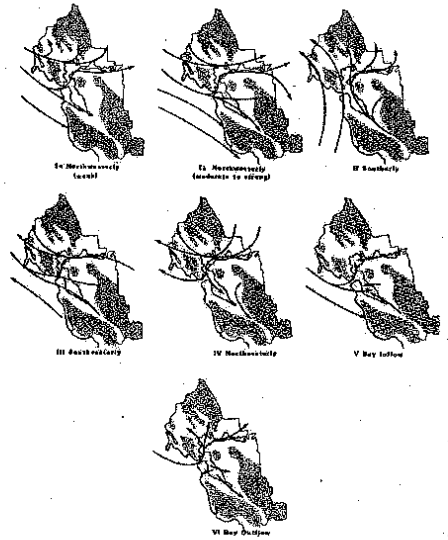

South Coast Air Basin

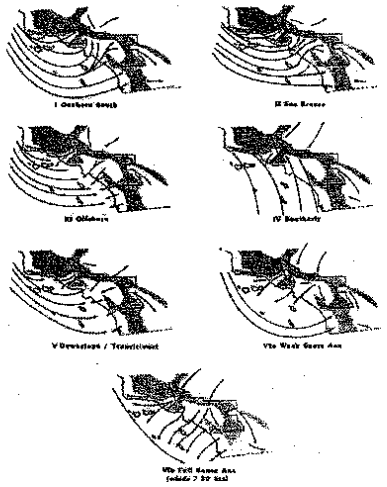

Period of Record: San Francisco International 1975-1979
Point Mugu NAS 1962-1977

Source: National Climatic Center

The air that flows around the Pacific high at upper levels sinks (subsides) and consequently warms due to air compression. This warm air above the cool coastal marine air produces a strong and persistent vertical temperature inversion that is a major influence on atmospheric stability. Atmospheric stability is the primary weather factor that influences the vertical dispersion of pollutants. In general, the more stable the air, the more dispersion is inhibited. An extremely stable subsidence inversion dominates the California coastal areas and effectively caps the marine layer, providing a ceiling above which pollutants cannot rise. This reduces the vertical dispersion of air pollution, particularly during the summer when the inversion is strongest and most persistent.

Table 4: Composite Surface Air Flow Types (1977-1981)

	San Francisco Bay Area Air Basin				South Coast Air Basin		
Season	**Onshore**	**Offshore**	**Calm**		**Onshore**	**Offshore**	**Calm**
Winter	59	25	14		38	45	16
Spring	88	7	5		64	27	9
Summer	96	1	3		73	16	11
Fall	80	10	9		53	34	13
Yearly	81	11	8		58	30	12

Source: California Air Resources Board , California Wind Climatology (June 1984)

Table 5 is a compilation of seasonal inversion frequencies and characteristics for Oakland, Vandenberg AFB, and Point Mugu NAS. The table shows that the mean height of the base of the subsidence inversions ranges between 600 and 2200 feet above sea level (asl) and is persistent throughout the year. (Inversions are present some 90 percent of the time.) The combination of a strong, persistent inversion and the onshore winds which characterize the coastal meteorology of California is conducive to the transport of offshore emissions to coastal air basins. Offshore emissions are transported beneath or within the inversion, with little dispersion, to onshore areas.

Table 5: Atmospheric Inversion Statistics 1975-1977

Oakland					
	Spring	Summer	Fall	Winter	Annual
Mean					
Invers. Top (ft asl)	3200	2800	2900	3000	3000
Invers. Base (ft asl)	2200	1200	1700	1900	1700
Strength	6	15	8	6	9
Percentage of Occur.					
Inversion	80	98	88	80	86
Base <= 3000' asl	58	94	71	60	71
Base <= 1000' asl	31	47	44	43	41
Vandenberg AFB					
	Spring	Summer	Fall	Winter	Annual
Mean					
Invers. Top (ft asl)	2900	3200	2700	2600	2900
Invers. Base (ft asl)	1700	1400	1400	1600	1500
Strength	10	20	12	8	13
Percentage of Occur.					
Inversion	89	99	93	85	92
Base <= 3000' asl	77	96	85	71	83
Base <= 1000' asl	40	32	50	55	44

Point Mugu NAS					
	Spring	Summer	Fall	Winter	Annual
Mean					
Invers. Top (ft asl)	1900	2800	2000	1400	2100
Invers. Base (ft asl)	1100	1300	1000	600	1000
Strength	7	14	10	8	10
Percentage of Occur.					
Inversion	84	99	96	87	92
Base <= 3000' asl	73	93	86	83	84
Base <= 1000' asl	57	47	66	68	59

Other Studies

Establishing the distance of how far offshore pollutants can be emitted and will have an expected onshore impact is dependent upon the models used and meteorology of the coastal area. For the development of emission inventories, U.S. EPA has investigated the extent to which emissions offshore have the potential to impact onshore air quality and taken that into consideration when developing emission inventories. Studies have also been conducted that investigate the over-water chemistry of ship emissions and how that may influence air quality models. In addition, information on the contribution of ship emissions impacts was evaluated from air monitoring data collected in Southern California during the strike of union workers at the Ports of Long Beach and Los Angeles. These are discussed briefly below.

For ocean-going vessels, the United States Environmental Protection Agency (USEPA) counts NOx emissions in their inventory if the vessel is operating within a 175 nautical mile boundary off of the United States coasts. (USEPA, 2003) As stated in the Support Document for Controlling Emissions from New Marine Engines at or above 30 liters per Cylinder, "this 175-mile area is based on the estimate of the distance a NOx molecule could travel in one day (assuming a 10 mile per hour wind traveling toward a coast, NOx molecules emitted 12 miles from the coast could reach the coast in just over one hour. NOx molecules emitted 175 miles, or 200 statue miles, could reach the coast in less than a day.)" Also mentioned in this report was a modeling study conducted by the Department of Defense That concluded that emissions released within 60 nautical miles of shore could make it back to the coast. (Eddington, 1997) In response to a request by the USEPA for comment on this 175-mile boundary, a study using 10 years of hourly surface wind data was performed to estimate the probability that offshore emissions will impact land from specified distances. (Eddington and Rosenthal, 2003) This study showed that for California, the probabilities were high (greater than 80 percent) that emissions from 50 nautical miles offshore will reach the coast within 96 hours.

There has been very little actual in-transit measurement of the pollutant emissions from ships to better understand various aspects of ship plume chemistry and reconcile differences between measurements and model predictions. However, a recent study conducted by Chen et al (Chen, 2005), where measurements of chemical species in ship plumes were taken from aircraft transecting a ship plume indicates that the NOx half-life within a ship's plume may be much shorter than predicted by photochemical models. The study demonstrated a NOx lifetime of about 1.8 hours inside the ship plume at noontime as compared to about 6.5 hours in the background marine boundary layer of the experiment. Additional studies investigating ship plume chemistry will help validate these results and help us better understand ship plume chemistry and improve the photochemical models used to investigate the impacts of ships on air quality.

Recently, a study was conducted that investigated ambient air quality data to examine contributions from ship emissions. In the fall of 2002, union workers at the ports of Los Angeles and Long Beach went on strike. The result was that the port operations shut down and about 200 ships were idling off the coast, immediately upwind of Long Beach. As part of a study in support of the University of Southern California Children's Health Study, researchers analyzed the effect of this strike on PM and gaseous pollutants at a monitoring site in Long Beach. Based on a comparison of PM and gaseous pollutant measurements from pre-, during and post-strike periods, they found statistically significant increases in particle number concentrations (60-200nm) and NOx and CO which they concluded are indicatives of contributions of emissions from the idling ships during the strike period. (ARB, 2005)

Conclusions

The transport of air pollution over long distances and between air basins has been well established. The emissions from ocean-going vessels can travel great distances and numerous studies have shown local, regional, and global impacts on air quality. Tracer studies, air quality modeling, and meteorological data analysis are typical approaches used to determine the extent to which emissions released offshore can impact onshore areas. Several studies support ARB staffs conclusion that emissions from ocean-going vessels released offshore the California Coast can impact onshore air quality.

REFERENCES

(ARB, 1982) *Air Quality Aspects of the Development of Offshore Oil and Gas Resources*; February 25, 1982.

(ARB, 1983) *Report to the California Legislature on Air Pollutant Emissions from Marine Vessels,* Volume 1; June 1983.

(ARB, 1984) *Report to the California Legislature on Air Pollutant Emissions from Marine Vessels*, Appendices H to M, Volume VII; June 1984.

(ARB, 2000) et al , *Air Quality Impacts from NOx Emissions of Two Potential Marine Vessel control Strategies in the South Coast Air Basin.*; November 2000.

(ARB, 2005) *Operation of SMPS and Low Temperature TEOM in Locations of the USC Children's Health Study (CHS) and the Los Angeles Supersite*, Final Report, Contract No. 01-300, April 2005.

(Acurex Environmental, 1996) *Marine Vessel Emissions Inventory and Control Strategies, Prepared for the South Coast Air Quality Management District*; December 12, 1996.

(ARCADIS, 1999) *Marine Vessels Emissions Inventory: Update to 1996 Report; Prepared for the South Coast Air Quality Management District*; September 23, 1999.

(Capaldo, Kevin, 1999) et al, *Effects of ship emissions on sulphur cycling and radiative climate forcing over the ocean*, Nature, Vol 4000; August 1999.

(Chen, G., 2005) et al, *An investigation of the Chemistry of Ship Emission Plumes During ITCT 2002*, Journal of Geophysical Research, Vol. 110, D10590, doi: 10.1029/2004JD005 2 36; 2005.

(Corbett, J.J. and Fishbeck, Paul, 1997) *Emissions from Ships*, Science, Vol 278; 1997.

(Corbett, J.J., and Koehler, H.W., 2003) Updated *emissions from ocean shipping*, Journal of Geophysical Research Vol. 108; 2003.

(Eastern Research Group and Starcrest Consulting Group, 2003) *Improvements to the Commercial Marine Vessel Emission Inventory in the Vicinity of Houston Texas*; July 28, 2003.

Endresen, 2003) O., et al, *Emission from international sea transportation and environmental impact*, Journal of Geophysical Research, 108; 2003.

(Eddington, Lee, 1997) *A Review if Meteorological Studies Pertaining to Southern California Offshore Ship Emissions And Their Effect on the Mainland*, Geophysics Branch, Naval Air Warfare Center Division, Point Mugu, CA., Geophysical Sciences Technical No. 200.; February 1997.

(Eddington, Lee and Rosenthal, Jay, 2003) *The Frequency if Offshore Emissions Reaching the continental UW Coast Based on Hourly Surface Winds from a 10 Year Mesoscale Model Stimulation*, Geophysics Branch Technical Note; March 2003.

(Fagerli, Hilde and Tarrasson, Lenonor, 2001) *The influence of ship traffic emissions on the air concentrations of particulate matter*. Oslo; November, 2001.

(International Maritime Organization, 2000) *Study on Greenhouse Gas Emissions from Ships*; March 2000.

(Jonson 2000), Jan E., et al, *Effects of international shipping on European pollution levels, Norwegian Meteorological Institute*, Research Report 41; July 2000.

(Lawrence, Mark G., and Crutzen, Paul J., 1999) *Influence of NOx emissions from ships on tropospheric photochemistry and climate*, Nature, 402; November 1999.

(Marmer, Ilina and Langmann, Baerbel, 2005) *Impact of ship emissions on the Mediterranean summertime pollution and climate: A regional model study*. Atmospheric Environment, 39; 2005.

(Murphy, T.) et al, *The Need to reduce Marine Shipping Emissions; A Santa Barbara Case Study*; Paper 70055

(Saxe, H. and Larsen, T., 2004) Air *Pollution from Ships in Three Danish Ports*, Atmospheric Enviroment, 38, 4057-4067; 2004.

(Streets, 2000) The *Growing Contribution of Sulfur Emissions from Ships in Asian Water, 1998-1995*, Atmospheric Environment, 34, 4425-4439; 2000.

(USEPA, 2003) *Final Regulatory Support Document: Control of Emissions from New Marine Compression-Ignitiion Engines at or Above 30 Liters per Cylinder*; January 2003

The Structure and Variability of the Marine Atmosphere around the Santa Barbara Channel

C. E. DORMAN AND C. D. WINANT

Center for Coastal Studies, Scripps Institution of Oceanography, San Diego, California

(Manuscript received 7 August 1998, in final form 10 February 1999)

ABSTRACT

The Santa Barbara Channel is a region characterized by coupled interaction between the lower-level atmosphere, the underlying ocean, and the elevated topography of the coastline. The nature of these interactions and the resulting weather patterns vary between summer and winter.

During summer, synoptic winds are largely controlled by the combined effect of the North Pacific anticyclone and the thermal low located over the southwestern United States, resulting in persistent northwesterly winds. A well-defined marine atmospheric boundary layer (MABL) with properties distinct from the free atmosphere above is a conspicuous feature during the summer. The wind has different characteristics in each of three zones. Maximum winds occur in the area extending south and east from Pt. Conception (zone 1), where they initially increase as they turn to follow the coast, then decrease farther east. Winds are usually weak in zone 2, located in the easternmost part of the channel, offshore from the Oxnard plain. Winds are also weak in zone 3, sometimes reversing to easterly at night, in a narrow band located along the mainland coast. Summer air temperature at the surface follows the SST closely and varies significantly with location. Summer sea level pressure gradients are large, with the lowest pressure occurring on the northeast end of the Santa Barbara Channel. Diurnal variations are strongest in summer, although the modulation is weakest in zone 1. The diurnal variation is parallel to the coast in all of zone 3 but the Oxnard plain, where it is perpendicular to the coast. The height of the marine layer varies between 300 m in late afternoon and 350 m in late morning.

In winter, synoptic conditions are driven by traveling cyclones and sometimes accompanied by fronts. These are usually preceded by strong southeast winds and followed by strong northwest winds. Atmospheric parameters are distributed more uniformly than in summer, and diurnal variations are greatly reduced. Sea level air temperature and pressure are more spatially uniform than in the summer.

Spatial variations in the observed fields in the summer are consistent with a hydraulic model of the MABL as a transcritical expansion fan. The summertime situation is governed by a coupled interaction between the atmosphere and the underlying water. The ocean influences the density of the MABL to the extent that it behaves distinctly from the free atmosphere above, resulting in strong winds polarized in the direction parallel to the coast. In turn, these winds provoke an upwelling response in the coastal ocean, which in part determines the surface properties of the water.

1. Introduction

The earliest account of the meteorological conditions in the Southern California Bight was made by Dana (1841), who described the strong southerly winds that could precede a frontal passage and were responsible for the grounding of ships against the lee shore of Santa Barbara. Ship-based climatology (Nelson 1977) reinforces the modern perception of coastal winds along the west coast of the United States: these winds are believed to be strong along the north coast and weak off southern California. Even more recent analysis of West Coast automated buoy winds revealed that there are two summer mean monthly wind speed maxima: one along northern California just north of San Francisco and the other at the western mouth of the Santa Barbara Channel (Dorman and Winant 1995).

Reports from automated buoys and ships show that the general open coast winds approaching Pt. Conception are from the northwest and stronger in the summer (Nelson and Husby 1983; Dorman and Winant 1995). Based upon land stations and experience, DeMarrias et al. (1965) suggested the afternoon sea surface winds sweep around Pt. Conception and along the Santa Barbara Channel, exiting mostly over the Oxnard plain or to the southeast toward Los Angeles (Fig. 1). In contrast, sea surface winds in the early morning along the north and east portions of the Santa Barbara Channel are light and variable. Wind direction along the coast and valleys is reversed so as to be from the land direction during weak, early morning, winter drainage winds. Aircraft

Corresponding author address: Clive E. Dorman, Center for Coastal Studies, Scripps Institute for Oceanography, San Diego, CA 92093-0209.

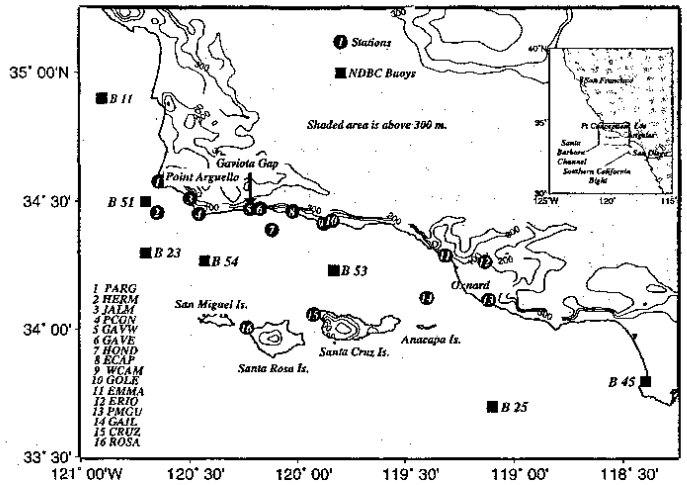

FIG. 1. Station locations and topography.

and buoy measurements show the acceleration of the sea surface winds around Pt. Conception into a maximum at the center of the western mouth of the Santa Barbara Channel (Brink and Muench 1986; Caldwell et al. 1986). Buoy, coastal stations, and finer-scale analysis of ship winds confirm that winds in the southerly and inner waters of the Southern California Bight are generally weak and westerly (Dorman 1982; Halliwell and Allen 1987; Dorman and Winant 1995).

During the extended summer, the area is dominated by a persistent, low, subsidence air temperature inversion caused by the northeastern Pacific anticyclone. Based upon limited observations, Neiburger et al. (1961) suggested that the inversion base over this area of the coast is around 400-m elevation, and the strength of the inversion is 10°C. The capped layer below is referred to as the Marine Atmospheric Boundary Layer (MABL). Aircraft observations in August–September 1966 showed that the inversion base was lowest at Gaviota (240 m), less that 350 m in the Santa Barbara Channel, and higher away from it, especially toward Los Angeles (Edinger and Wurtele 1972). The depth of the marine layer at the coast can vary from 0 to 800 m (e.g., Edinger 1959, 1963; Baynton et al. 1965; Dorman 1985a; Wakimoto 1987).

The South Central Coast Cooperative Aerometric Monitoring Program (SCCCAMP) took place for 5 weeks in September and October 1985 (Dabberdt and Viezee 1987) to monitor air pollution events. A review of background measurements and four intensive measurement periods points out synoptic and mesoscale patterns associated with high ozone. These patterns include a cyclonic eddy centered in the Santa Barbara Channel and an eddy at Gaviota (Douglas and Kessler 1991; Hanna et al. 1991). A numerical study by Kessler and Douglas (1991) found that a combination of steep topography and diurnal heating with cross-ridge flow results in trapping and westward phase progression of wind direction shifts along the south slopes of the mountain behind Santa Barbara.

Certain synoptic situations force locally distinct responses. Santa Anas are gusty, offshore, warm, dry winds that occur from autumn to spring when high pressure is situated over the Great Basin of Nevada and Utah (Sommers 1978). Santa Anas are usually strong at the mouths of river valleys. The reach of the offshore surface winds is believed to be limited but may extend to the distant islands in extreme cases (DeMarrias et al. 1965).

A cyclonic eddy within the marine layer covering the Southern California Bight may occur at any time of the year and is usually associated with an elevated air temperature inversion base and a stratus overcast (e.g., Rosenthal 1968, 1972; Bosart 1983; Dorman 1985a; Wakimoto 1987; Mass and Albright 1989; Clark and Dembek 1991). It has been a local custom to refer to all such features as "Catalina eddies," but different events may be associated with different causes and dynamics.

The interaction of synoptic-scale features with the topography and the stable marine layer may result in topographically trapped events. At the very least, this interaction contributes significantly to the topographic trapping of the dynamics of the response. There has been considerable discussion about whether there might be solitary Kelvin waves or gravity currents present (e.g., Dorman 1985a, 1987; Mass and Albright 1987; Wakimoto 1987; Clark and Dembek 1991; Eddington 1985; Eddington et al. 1992; Reason and Steyn 1992). There

TABLE 1. Stations.

Designator	Station	Lat N	Lon W	Elev (m)	Variables	Operator
B11	Buoy 46011	34°54′	120°54′	0	W, T_a, T_s, P	1
B23	Buoy 46023	34°18′	120°42′	0	W, T_a, T_s, P	1
B25	Buoy 46025	33°42′	119°06′	0	W, T_a, T_s, P	1
B45	Buoy 46045	33°48′	118°24′	0	W, T_a, T_s, P	1
B51	Buoy 46051	34°30′	119°42′	0	W, T_a, T_s, P	1
B53	Buoy 46053	34°14′	119°50′	0	W, T_a, T_s, P	1
B54	Buoy 46054	34°16′	119°26′	0	W, T_a, T_s, P	1
CRUZ	Santa Cruz Island	34°04′	119°56′	20	W, T_a, P	2
ECAP	El Capitan	34°28′	120°01′	39	W, T_a	3
EMMA	Emma Woods Beach	34°17′	119°19′	3	W, T_a	4
ERIO	El Rio	34°16′	119°08′	34	W, T_a	4
GAIL	Gail Platform	34°08′	119°24′	30*	W, T_a, P	2
GAVE	Gaviota East	34°28′	120°11′	34	W, T_a	3
GAVW	Gaviota West	34°28′	120°13′	29	W, T_a	3
GOLE	Goleta	34°26′	119°50′	3	W, T_a, RP	5
HOND	Hondo Platform	34°23′	120°07′	44*	W, T_a, P	2
JALM	Jalama Beach	34°31′	120°30′	6	W, T_a	3
HERM	Hermosa Platform	34°27′	120°39′	40*	W, T_a, P	2
PARG	Pt. Arguello	34°35′	120°38′	52	W, T_a, P	1**
PCON	Pt. Conception	34°27′	120°27′	55	W, T_a	3
PMGU	Pt. Mugu NAS	34°07′	119°07′	4	W, T_a, P	6
ROSA	Santa Rosa Island	34°00′	120°14′	17	W, T_a, P	2
WCAM	West Campus	34°25′	119°53′	9	W, T_a	3

W = winds, T_a = temp air, T_s = temp sea, P = pressure, RP = radar profiler.
* = anemometer height.
** = CMAN station.
1 = National Data Buoy Center.
2 = Scripps Institution of Oceanography.
3 = Santa Barbara Air Pollution Control District.
4 = Ventura Air Pollution Control District.
5 = NOAA, ETL, Boulder.
6 = U.S. Navy.

has also been the suggestion that part of the formation phase of some Catalina eddies might involve trapping.

The Center for Coastal Studies at Scripps Institution of Oceanography has been involved in a multiyear oceanographic program on the Santa Barbara Channel sponsored by the Minerals Management Service. Part of this program included making automated surface measurements and retrieving other measurements obtained by air pollution control districts. The result is an extensive network of surface stations (Fig. 1) with limited upper-air measurements. The object of this paper is to describe the atmospheric conditions in and around the Santa Barbara Channel and to examine the possible underlying dynamics.

2. Observations

The Santa Barbara channel is approximately 40 km wide and 100 km long (Fig. 1). The coastline at Pt. Conception near the northwestern edge of the channel is sharply curved, directed meridionally north of Pt. Arguello and zonally to the east of Pt. Conception. The north side and east end of the Santa Barbara Channel is lined with topography that extends abruptly to well above 300 m. On the east end, the low Oxnard plain forms the mouth of a river valley that extends upward and to the northeast. Lining the south side are the four Channel Islands: San Miguel, Santa Rosa, Santa Cruz, and Anacapa. The center two islands extend above 400 m. Gaps exist between the islands, which can act as wind funnels. Surface air exiting the southeast end of the channel may continue to the greater Los Angeles basin, to the southeast.

There are 21 automated surface meteorological observation networks used for this analysis. Scripps Institution of Oceanography (SIO) maintained three automated stations on oil platforms and two on islands (Fig. 1, Table 1). The National Data Buoy Center (NDBC) made hourly observations from six buoys and one coastal station (Hamilton 1980). Hourly coastal automated observations were also available from six Santa Barbara Air Pollution Control District stations and two Ventura Air Pollution Control District stations. Finally, hourly data was provided by the U.S. Navy at Pt. Mugu. The SIO and air pollution control stations data are averaged over the hour. The NDBC and Pt. Mugu stations are an average of several minutes near the hour. Winds and air temperature were measured at all stations. Pressure was recorded for the SIO and NDBC stations and Pt. Mugu. Sea temperatures were taken only at the NDBC buoys.

The atmospheric pressure at all stations was adjusted

to sea level as described by Dorman and Winant (1995). Buoy winds were adjusted to 10 m above sea level following the method described by Large and Pond (1981) for a neutral atmosphere. Winds from oil platforms were not adjusted owing to the uncertainty of the effect of the platform structure on the wind field, which can be positive or negative (Thornthwaite et al. 1965). HERM (see Table 1 for station name definitions) wind observation at 40-m elevation is similar in magnitude to the nearby NDBC buoy 51 (B51) wind observation at 10 m. No adjustments were made to the coastal or island station winds.

Vertical profiles are from three different instruments. The National Oceanic and Atmospheric Administration Environmental Research Laboratory (Boulder, Colorado) maintained a radar profiler at Goleta from May to September 1996. This station is on a low coastal plane on the north side of the Santa Barbara airport, 2 km from the ocean. The radar profiler provided hourly vertical profiles of horizontal winds at 100 m vertical spacing. Hourly, consensus-averaged winds, which are used here, were calculated from measurements made every few minutes with some limited intervals of interference from birds removed. Vertical profiles of a virtual temperature, assumed to be the air temperature, were constructed from a radio acoustic sounding system that is operated in conjunction with the radar profiler. Details about the radar profiler, radio acoustic sounding system, and averaging techniques are described by Ralph et al. (1998).

A U.S. Navy–sponsored Variability of Coastal Atmospheric Refractivity (VOCAR) field program operated eight land-based, upper-air sounding stations over the Southern California Bight from 23 August to 3 September 1993 (Paulus 1995). One of these was a tethered balloon station at Gaviota on the low, narrow coastal plain at 60-m elevation and 600 m from the ocean. Here, 2-hourly tethered balloon soundings were made for a 3-week period ending on 3 September 1993. Surface data variations during VOCAR are described in Fisk (1994).

3. Overview

Averages based upon multiyear analysis of buoy winds over southern California coastal waters suggest that May–July and December–February are representative of summer and winter while the other months are transitional (Dorman and Winant 1995)—a scheme that we adopted for this paper. A 2-yr time series for two stations for December 1995–November 1996 is shown in Fig. 2 to give an overview of the annual and synoptic-scale variability. The plotted winds are rotated into components along and across the direction of maximum variance based upon a year's observations (the principal axis or PA). Buoy 54 is typical of the faster wind speed stations in the western mouth. It has more direction reversals in the winter than in the summer due to the stronger synoptic events in the winter. Summer winds are more persistently from a northerly direction but still have large variations in magnitude. Other overwater stations have similar annual structure but synoptic-scale variations of lesser magnitudes.

The north coastal stations generally have weak winds, and those in the western half are punctuated by spikes in the wind speed. Typical of this group is ECAP, which has dominantly weak, along-coast variations with little seasonal trend. Cross-coast, reversing wind pulses of short duration occur mostly in the winter. Offshore-only pulses happen mostly between March and June.

The scalar variables of pressure, air temperature, and sea surface temperature (SST) are shown only for B54, which is representative of the other stations. Maximum pressure variability is associated with winter synoptic-scale variations. Minimum pressure and variability are in the late summer when synoptic variations are greatly weakened and the large-scale North Pacific anticyclone retreats to its most northern position. Sea temperature is a weak minimum in the early summer to midsummer, reflecting the dominance of wind-driven, coastal upwelling. The air temperature is held close to that of the sea as a persistent, dense atmospheric marine boundary layer is present. The marine layer is isolated from exchange with air above by an air temperature inversion and from horizontal exchanges with inland extremes by topography. The layer's dominant thermal contact is via long trajectories over the sea, which has a large heat capacity. The result is that the mean monthly sea minus air temperature at B54 (not shown) has a difference of −0.6°C in April and a maximum of 1.3°C in September.

A distinct annual trend is seen in the monthly mean wind vectors at the western end of the Santa Barbara Channel and Pt. Conception area (Fig. 3). The strongest speeds are in the summer (maximum is April and May 1996) and weakest in the winter (minimum is February 1996) but always from a northwesterly direction. The annual trend has similar annual phase but much weaker magnitude in the eastern end of the channel. Stations on the north channel coast and east of Pt. Conception, with the exception of Ventura (EMMA), have weak means with no significant annual speed trend that is typified by GAVE and WCAM.

The remainder of this paper is organized around examining the two representative seasons. The summer structure and variations are presented first. This is followed by a description of the winter structure. Next is a section on the offshore winds at Gaviota and eddies in the wind field. This is followed by a discussion of dynamics based on the earlier portions of this paper.

4. Summer structure and variations

a. Mean fields

Maps of the mean wind and principal axes (PA) direction and strength are shown in Fig. 4 for May–July

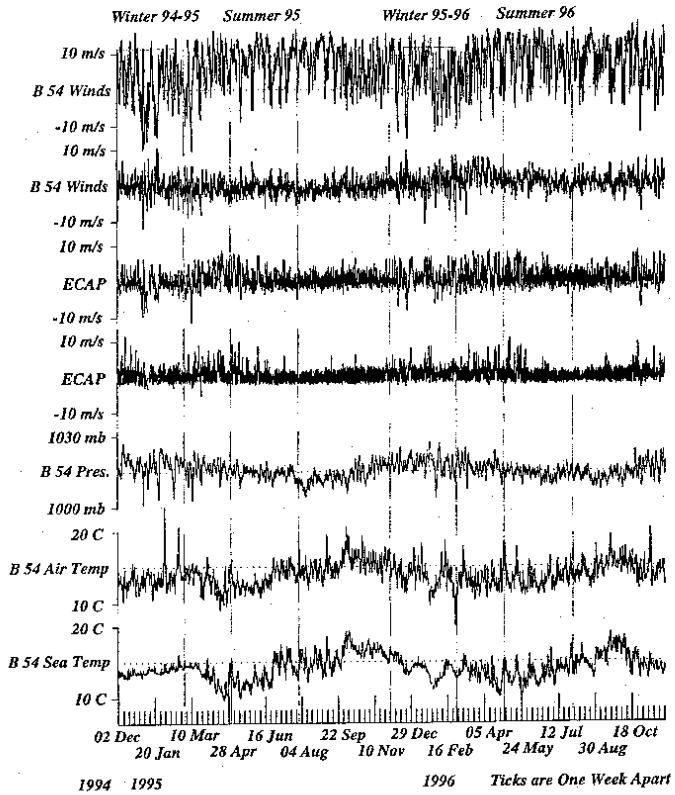

FIG. 2. Winds along and across the principal axes for B54 and ECAP. Pressure, air temperature, and sea temperature is for B54. The top frame is the B54 major axis of the wind (along 306°T), the second frame is the B54 minor axis (along 216°T), the third frame is ECAP winds along the major axis (along 311°T), and the fourth frame is ECAP winds along the minor axis (along 221°T).

1996 (values in Table 2). B23 and JALM were not available for this period, so averages for May–July 1995 have been substituted.

The sea level winds approach the channel from the northwest, accelerate, and turn cyclonically around Pt. Arguello, reaching a maximum in the middle of the western channel (Fig. 4). Once past this point, the near-surface air slows as it continues down the center of the channel, exiting to the east into the Ventura Valley or continuing over water to the southeast toward the greater Los Angeles Valley. Compared to the center channel, winds are weaker at the islands on the south edge and very weak along the northern coast east of Pt. Conception. Standard deviations are less than the means for the overwater stations in the western mouth but much larger than the weak means along the north side, which are east of Pt. Conception and the overwater stations on the east end.

The Santa Barbara Channel stations may be divided into three zones according to the character of the wind variations. Station B54 is typical of zone 1, where stations have a high velocity and strong polarization with winds dominantly from a north-northwest direction (Fig. 5). At B54 during the summer of 1996, 84% of the days had winds greater than 10 m s^{-1} for part of the day, 67% of the days had winds from 306° (also along the PA) greater than 5 m s^{-1} for the entire day, 16% had winds in the same direction but between 0 and 5 m s^{-1}, while 19% had winds from 126° for part of the day.

At B53, 22% of the days had winds from the west along the PA greater than 10 m s^{-1} during part of the day, 34% of the days had winds that were from 80°

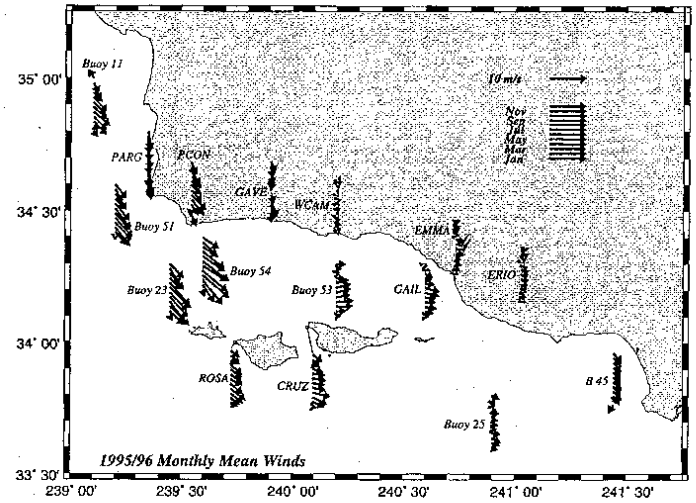

FIG. 3. Wind vector mean monthly annual trend. Monthly mean winds for Jan (lowest arrow) through Dec 1996 (uppermost arrow). Speeds are greatest in the western channel mouth in the summer.

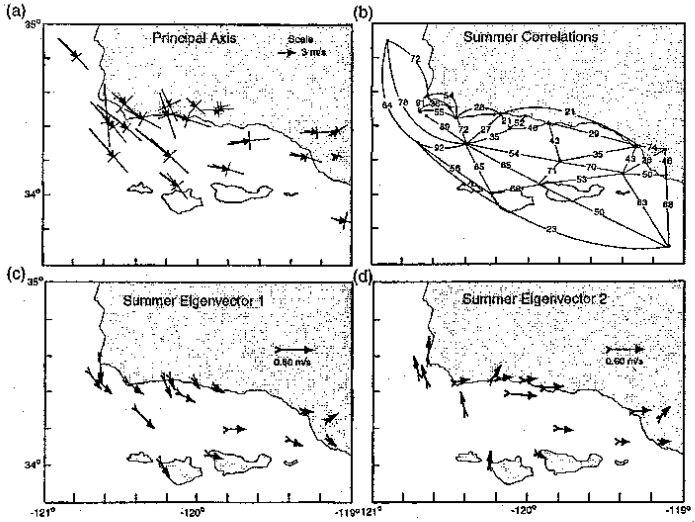

FIG. 4. (a) Summer mean surface wind speed and principle axes (PA). The arrow that flies with the wind represents the mean. The cross at the end of the wind vector is the wind standard deviation with the long side the maximum magnitude and orientation and the short side the minimum. (b) Summer wind correlations along station PAs. (c) and (d) First and second empirical orthogonal functions for the summer.

TABLE 2. Station wind characteristics.

Station	Mean speed (m s^{-1})	Mean direction (deg)	PA direction (deg)	Major axis speed (m s^{-1})	Minor axis speed (m s^{-1})	Speed difference (m s^{-1}; 16–08 PST)
			Summer			
B11	5.2	136	139	3.4	1.2	1.4
B23	7.3	139	138	4.1	1.5	0.7
B25	1.8	96	101	2.9	1.8	2.9
B45	2.5	138	120	2.0	1.8	2.3
B51	6.6	138	142	3.9	1.2	0.0
B53	4.3	80	86	3.8	1.8	3.4
B54	8.7	128	133	5.0	1.7	1.8
Cruz	4.1	84	92	3.2	1.4	2.2
ECAP	0.5	120	131	2.4	1.8	1.1
EMMA	2.5	97	88	3.4	1.3	4.1
ERIO	1.4	60	59	2.2	0.9	3.2
GAIL	3.2	98	107	3.2	0.9	2.8
GAVE	0.4	173	155	3.4	2.3	1.1
GAVW	2.6	160	161	4.8	2.0	1.5
HERM	7.5	129	131	3.9	1.3	1.0
HOND	2.0	114	108	4.9	1.8	4.6
JALM	1.6	145	133	3.5	2.4	2.7
PARG	7.8	176	175	4.7	1.4	1.3
PCON	4.1	127	119	4.0	1.7	4.5
PMGU	0.9	81	107	1.1	0.8	1.8
ROSA	4.3	111	126	3.2	1.5	1.3
WCAM	0.7	63	86	2.9	1.5	1.5
			Winter			
B11	0.8	153	142	5.9	2.4	0.8
B23	4.3	142	131	6.4	2.5	0.7
B25	1.8	120	103	4.3	2.6	0.5
B45	1.6	140	108	3.2	2.5	0.9
B51	3.5	149	132	6.6	2.2	0.4
B53	1.9	89	98	5.3	2.1	1.4
B54	4.2	134	123	6.8	2.6	0.7
CRUZ	2.4	111	107	5.0	2.6	1.4
ECAP	1.1	175	116	2.7	1.7	0.7
EMMA	1.2	179	85	3.6	1.7	0.5
ERIO	0.9	191	63	2.7	1.5	0.0
GAIL	1.3	93	115	4.6	1.7	1.6
GAVE	1.2	188	125	3.5	2.1	0.7
GAVW	3.0	167	140	4.2	2.1	2.7
HERM	3.3	136	129	6.2	1.9	1.4
HOND	1.6	142	112	5.4	2.0	2.0
JALM	1.7	71	105	2.9	2.1	2.3
PARG	3.6	175	165	6.7	2.1	0.4
PCON	2.3	155	119	5.0	1.9	0.9
PMGU	0.1	118	108	1.3	0.9	0.4
ROSA	2.9	114	112	4.0	2.1	1.1
WCAM	0.7	158	95	2.8	1.7	0.6

greater than 1 m s^{-1} for part of the day. On only 8% of the days did B53 have any winds from 260° greater than B54 had from 306°. Other stations in this zone are the northern mouth stations of Pt. Arguello, Hermosa, B51, Pt. Conception, and the island stations of SROS and SCRZ.

Zone 2 is in the eastern end of the channel, adjacent to the Oxnard plain. This zone has the single station of GAIL, which has two different major wind alignments (Fig. 5). The dominant daily winds were from 280°, which occurred 74% of the summer days, while the winds greater than 1 m s^{-1} for at least 3 h from 135° occurred on 25% of the summer days. However, only 1 day had afternoon winds from 135° for greater than 3 h. As will be discussed later, this does not support the dominance of a midchannel eddy. On 23% of the summer days, both GAIL and B53 had a component from the east-southeast in excess of 1 m s^{-1}.

Zone 3 stations are along the north and east coast. They have a diurnally reversing wind direction. For the stations from GAVE to EMMA, the dominant wind alignment along the coast is generally from the west in the afternoon and the east in the night and early morning. GAVE winds are mostly parallel to the coast, with some scatter from the northwest that exceeds 10 m s^{-1} (Fig. 5). HOND, just 6 km offshore, has stronger along-

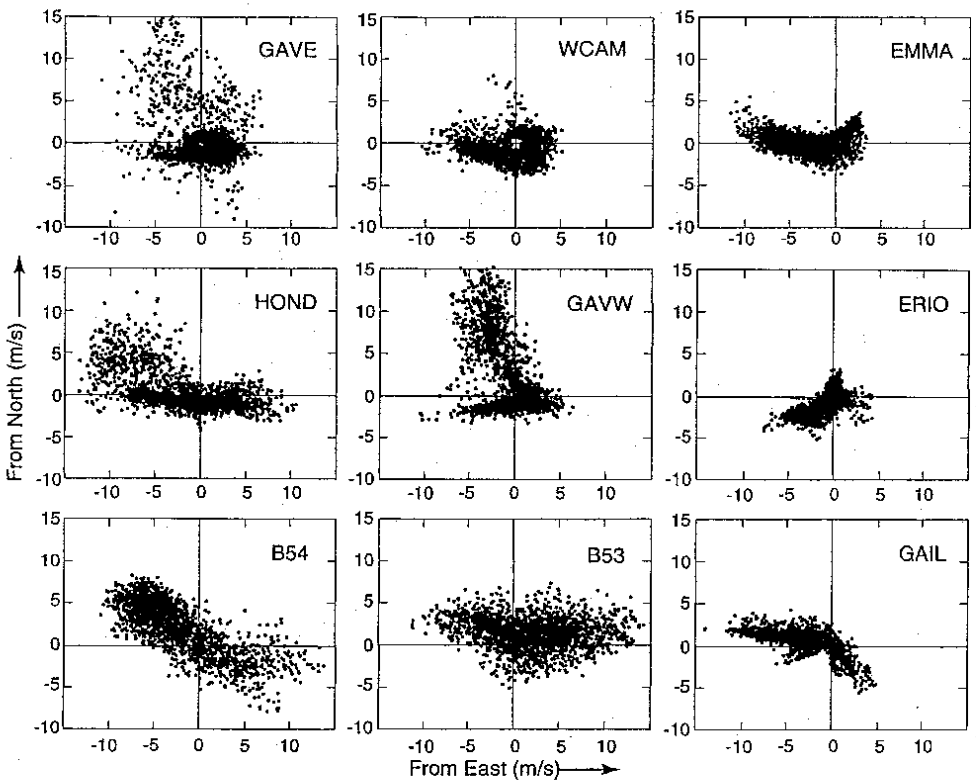

FIG. 5. Scatterplots of summer winds at representative stations. All summer wind hourly observations for a station are plotted relative to true north. Fastest mean winds and greatest polarization is at B54.

shore winds from either direction than GAVE or GAVW. WCAM has weaker alongcoast winds that are a little stronger from the west but lack the minority cases of strong offshore component experienced by the more western coastal stations. EMMA has no strong offshore component, but the westerly component is faster than the easterly component. ECAP and JALM are similar to GAVE (not shown). GAVW has two dominant modes: one is the alongshore, diurnally reversing mode and the other GAVW mode is a strongly polarized, high speed, offshore wind.

ERIO, on the Oxnard plane, experiences a diurnally reversing, cross-coast sea/land breeze as air moves up or down the Ventura River valley. The weak, semidiurnal speed maximums are in 2–4 m s^{-1} range and are generally unrelated to the dramatic speed changes in the western mouth such as at B54. Not included in zone 3 are PARG and PCON, which are on low points of land that extend out beyond the narrow coastal plane and have wind characteristics of zone 1 (stronger winds polarized from the north or northwest and not diurnally reversing along coast).

There is a distinct asymmetry with lower pressure on the north side (Fig. 6), in the cross-channel pressure field for the mean summer sea level pressure. The pressure field is lowest in the eastern end of the channel and even lower toward Los Angeles (not shown). There is a small pressure maximum around Pt. Arguello that may be associated with a thickened marine layer and increased clouds.

b. Correlations and EOFs

Correlations for the summer season were computed among the stations for the wind along the PA (Fig. 4). The best correlations (0.7–0.9) are between the zone 1 stations in the western mouth of the channel (B54 with others). Weak correlations (0.5–0.6) are between the western mouth (as represented by B54) and the eastern central stations as B53 and CRUZ. Poor correlations

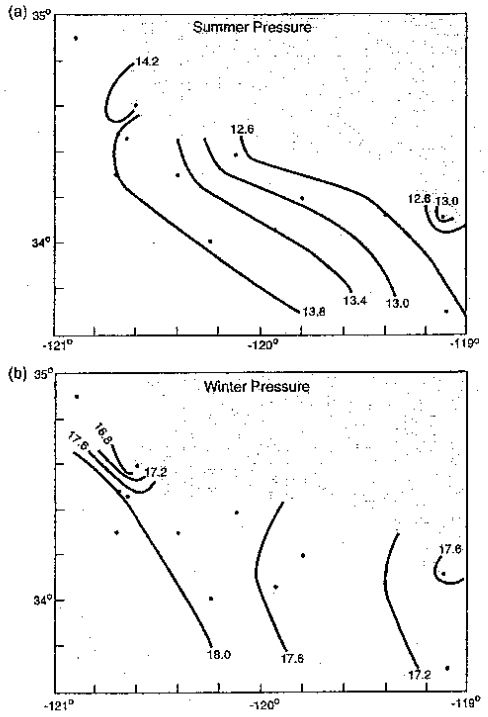

FIG. 6. (a) Summer and (b) winter mean sea level pressures (hPa). A cross-channel gradient occurs only in the summer.

exist between the center line channel stations (B54, B53) and the land coastal stations (GODW to EMMA and HOND). Even though it is over water, HOND is poorly related to B54 as well as the coastal stations. In contrast, the two stations on exposed points (PARG and PCON) are moderately correlated with the near, overwater stations (B54, HERM).

The covariability of the horizontal structure of the surface wind field was examined by EOF analysis (Lorenz 1956). A separate analysis (Fig. 4) was done for the summer (May–July 1996) and winter (December 1995–February 1996). The weight of the first three modes of each season are significantly different (Table 3). The eigenvector patterns are similar for the summer and winter. Eigenvector 1 is all in an east–west direction, with the largest values in the western mouth. This mode is associated with the dominant, synoptic-scale variations seen in both the summer and the winter.

Eigenvector 2 is oriented north–south in the western mouth and east–west in the eastern half. This mode is associated with diurnal variations that are also important in all seasons. This is a formal confirmation of an earlier noted observation: the majority of the land stations

TABLE 3. Eigenvector weights.

Summer EOF		Winter EOF	
Mode	Weight	Mode	Weight
1	0.44	1	0.65
2	0.18	2	0.09
3	0.10	3	0.44

(zone 3) scatterplot winds are along coast. On the other hand, the western mouth stations (SROSA, B54, B51/HERM, and PARG) are at right angles to the eastern half and the coastal land stations in the channel. The effect is that the eastern station component is from the west while the western is from the south, creating a zone of divergence between the two. If both sets of stations are reversed, there will be a zone of convergence between the two.

The strongest and most significant values for eigenvector 3 (not shown) are for the central, north-coast stations that have a strong, cross-shore, northerly component. This is associated with the lee events and cross-coast wind events that are mostly seen at GAVW, GAVE, and HOND.

Time series of the first two EOF modes are shown in Fig. 7 for summer and winter. The first mode is dominated by synoptic-scale variations of the order of 10 days' duration. The second mode is dominated by diurnal variations. The variation of both time series is similar in magnitude and period for the summer and winter seasons.

c. Synoptic variability

The most frequently occurring summer event is high speed, sustained winds from the northwest followed by a short period of weak winds. Fastest winds are at the western mouth of the Santa Barbara Channel and are associated with strengthened along-coast sea level pressure gradient and weak cyclonic circulation in the mid-level of the atmosphere. A typical case is shown for the period 2–10 July 1996. The main sea level synoptic features are the North Pacific anticyclone to the northwest (to the northwest of the area shown in Fig. 8) with a heat low in the southwest United States. North of Pt. Conception, the along-coast pressure gradient strengthens from 3 to 5 July then decreases again on 9 July as the heat low expands. Sea level pressure gradients over water are consistently weak southeast of Pt. Conception for the entire period despite the variation in sea level speeds at the western mouth (Fig. 9). At 700 hPa (not shown) an approaching trough on 3 July weakens as it moves over the California coast on 7 July and to eastern California on 9 July.

The sea level winds in zone 1 respond to synoptic variations. Examples of selected stations are shown in Fig. 9 (the wind direction has been rotated to the station's PA so as to make viewing easier). After a brief

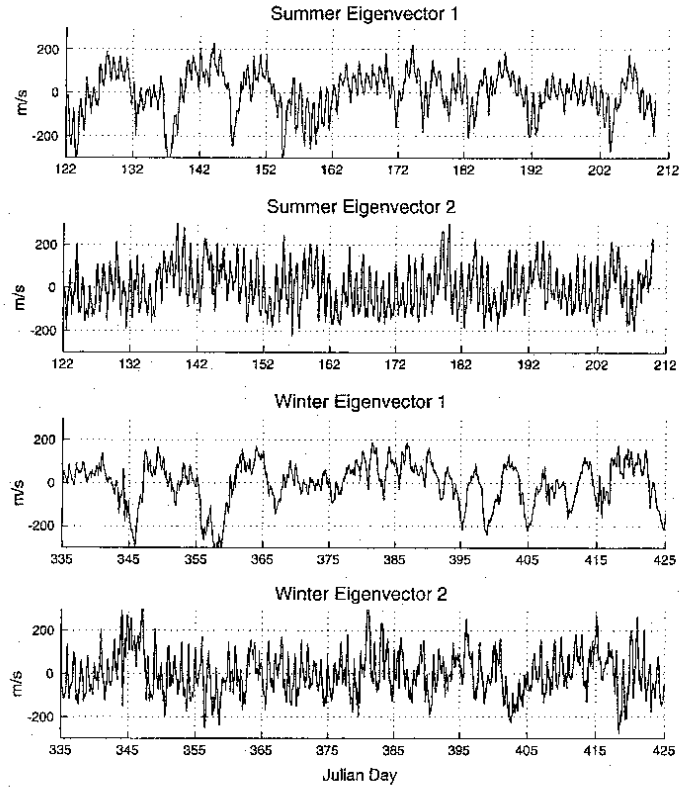

FIG. 7. Time series of the first and second eigenvector modes of the winds for the summer and the winter. The synoptic scale dominates the first mode and the diurnal scale is predominant in the second.

period of weak winds, strong inbound northerly winds persisted at B51 for 7 days with stronger winds at B54. Once past B54, wind speeds decrease to B53, then to GAIL (not shown), to reach a minimum speed at ERIO in the eastern end. Indeed, it would be hard to determine the state of the winds at the western mouth of the SB channel if only the El Rio observations were available. Winds at the channel islands (SROS and SCRZ, not shown) are somewhat weaker but correlated with the buoy winds at B54 and B51. The winds over the zone 3 land stations were generally west–east with only an occasional clear, cross-coast, northerly velocity such as occurred at GAVE (and GAVW and HOND) for 4 h early on 5 July. While it is the local custom to call such offshore events "sundowners" (Ryan 1996), the wind was observed only in the immediate area of GAVW, which is at the foot of the ridge height minimum of the Santa Ynez mountains. The next event was weak winds and reversals on 9–10 July, becoming the second most frequently occurring event over the open channel.

d. Diurnal variability

Generally, all winds are strongest in the early afternoon and weakest around sunrise. The zone 3 coastal land stations in Fig. 4 have weak, along-coast winds that are diurnally reversing. The exceptions are ERIO and PMGU, where the winds are cross-shore. The strongest wind reversals are at the land stations of HOND and EMMA. The eastward flow decreases and diurnal range increases from B54, to B53, to GAIL, to ERIO. The diurnal character is substantially different for the easternmost station on the Oxnard plane, which has a maximum between 1100 and 1600 PST and reverses direction to weakly offshore at night (2100–0700 PST).

Summer temperatures are for the May–July 1996 pe-

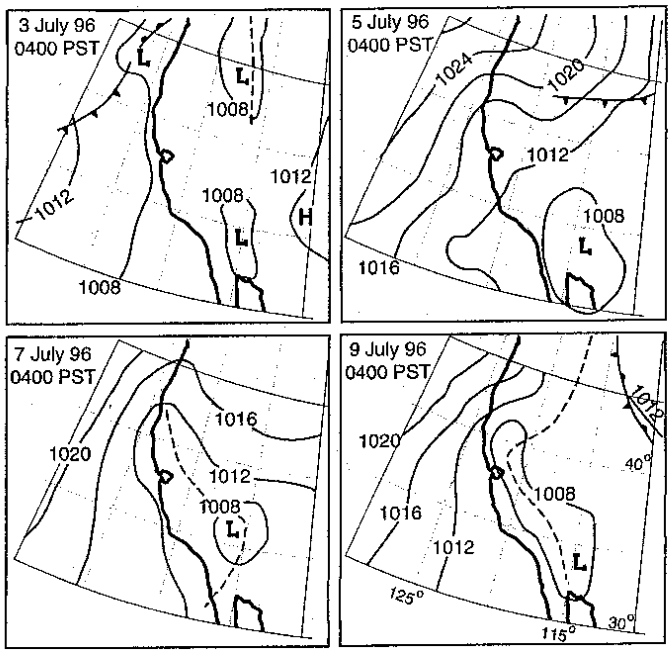

FIG. 8. Sea level pressure analysis (hPa) for Jul 1996. PST is Pacific Standard Time (UTC minus 8 h).

riod for all stations except B11, PARG, and JALM, for which May–July 1995 has been substituted (Fig. 10). In the summer morning, the land is warmer than the sea in the Santa Barbara Channel, with a weak gradient to the east. In the afternoon, all stations are warmer, with the weakest increases over the western mouth and the greatest over the land at the eastern end. Added to the 0600 PST chart are thin dashed lines representing the seasonal averaged SST contours from satellite infrared images. Wind-driven upwelling, associated with the fastest winds, causes the SST minimum in the western mouth (Harms and Winant 1998). The air temperature field is similar to the SST field due to the low heat capacity of the air and the restricted exchange of the marine air with other sources.

A radar profiler operating at Goleta for June and July of 1996 shows three distinct layers and considerable diurnal variation in the structure below 1000 m. The air temperature inversion base is a minimum of 170 m between 2100 and 0100 PST and a maximum of 320 m at 1000 PST (Fig. 11). A similar elevation change trend is followed by the air temperature inversion top with a minimum of 820 m and a maximum of 1070 m. In the air temperature inversion, the strongest winds are offshore at night and the early morning. In the morning, the vertical thermal structure is a marine layer capped by a low air temperature inversion base near 200 m and an air temperature inversion top at 1000 m. In the shallow marine layer, the winds are mostly from the east and weakly onshore. In contrast, the wind in the air temperature inversion is cross shore, from the north. Above the inversion top, winds are from the east. By the middle afternoon, the weakly onshore surface layer is predominantly from the west, while it has reversed to southerly in the air temperature inversion. Above the air temperature inversion top at 1000 m, the winds remain easterly but increase in speed with elevation.

The diurnal phase relationships between Goleta temperature inversion base height and winds are distinct and clearly repeated on most summer days (Fig. 12). In the late morning, the marine layer thickens and the surface winds are westerly while the inversion winds turn southerly. In the early evening, after sunset, the marine layer thins and the surface winds reverse to easterly while the inversion winds are from the north.

The diurnal air temperature inversion base height phase and amplitude at Goleta is similar to that at Gaviota 34 km to the west. During the VOCAR 3-week sounding session in August–September 1993, 2-hourly tethered soundings were made to 1 km. It was found at

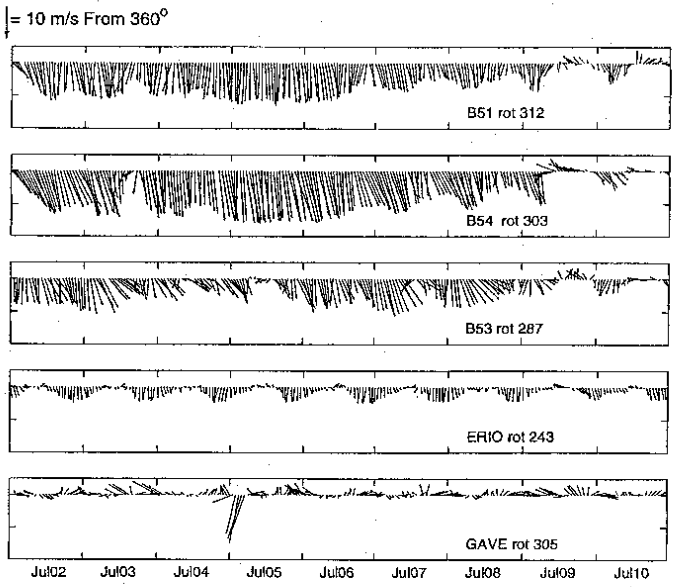

FIG. 9. Surface wind vector time series rotated to the PA for 2–11 Jul 1996 for selected stations.

Gaviota that winds in the lowest 100 km were mostly east–west, while those above could be appreciably cross-shore. Thus, the simple model of cross-coast, diurnally reversing land–sea breeze clearly does not apply here.

e. Larger bight marine-layer structure

We present here a synopsis of the results of the Navy VOCAR sounding program that maintained eight upper-air stations in the Southern California Bight in August and September 1993. In the morning at 0400 PST, the inversion base was lowest in the Santa Barbara Channel and highest in the southern half of the bight (Fig. 13). The strength of the inversion is greater offshore. In the afternoon, at 1600 PST, all base heights are typically about 100 m lower but the lowest is still in the Santa Barbara Channel. The strongest horizontal gradient in the inversion base height is at the western mouth of the Santa Barbara Channel. The greatest inversion strength is to the southwestern portion of the bight while it is weakest in the Santa Barbara Channel.

f. Summer satellite cloud cover

Summer clouds over the ocean in this area are mostly stratus that are restricted to the marine layer. Since the amount of stratus tends to increase with the marine-layer depth (Rosenthal 1972), the amount of cloud cover should be a relative indicator of the marine boundary layer depth. To investigate the cloud structure, the albedo of *GOES-9* visual images were averaged by hour for May–July 1996. The results shown in Fig. 14 are the percent albedo such that 100 would mean a cloud overcast 100% of the time. There is a generally decreasing trend in cloud cover after sunrise that is represented by the hours of 0800, 1200 (not shown) and 1600 PST. At 0800, there is the greatest cloud cover over the water. The marine layer extends across the coastal plains and lower portion of the river valleys, extending the clouds inland to the north of Pt. Arguello, the Oxnard plain, and the coastal plains to the south of Los Angeles. The least clouds are in the lee of Pt. Arguello/Pt. Conception and the western mouth of the Santa Barbara Channel. There is lesser cloud cover over or around all islands, some of which project above the average marine-layer depth. The Channel Islands have a larger area of decreased cloud cover in the lee.

By 1200 PST (not shown), the clouds have greatly decreased in the California Bight and a narrow coastal clear strip to the north. The clear areas in the lees of Pt. Arguello and the Channel Islands have expanded. The largest continuous low cloud area is in the inner coastal zone south of Los Angeles, reflecting the strong subsidence under the returning sea breeze circulation.

At 1600 PST, the low cloud area in the lee of Point

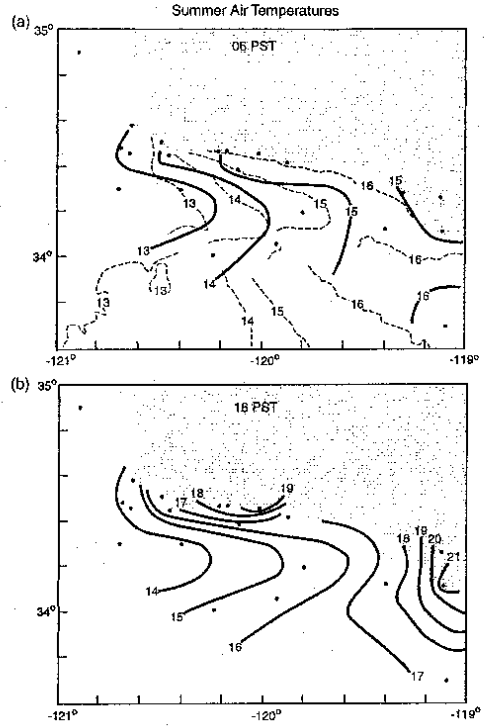

FIG. 10. Summer mean air temperatures (°C) at (a) 0600 PST and (b) 1400 PST. It is coolest in the western mouth. The summer SSTs estimated from satellite infrared images are superimposed on the upper chart as thin dashed lines.

Arguello has extended to all of the Santa Barbara Channel, the Channel Islands lee, and has connected to over water, low cloud areas to the east and southeast. Still, the absolute lowest cloud cover is in the immediate lee of Pt. Arguello and coastline of Santa Barbara Channel and the Channel Islands. Against the trend, cloud cover increased as the marine layer thickened at the coast north of Pt. Arguello. There was also an increase on the northwestern ends of each of the Channel Islands. The summary is that the marine clouds have considerable horizontal structure and a strong diurnal trend over the Southern California Bight. Nevertheless, the marine clouds tend to appear the least in the western mouth of the Santa Barbara Channel throughout the day, and, by inference, the lowest marine layer throughout the day.

The cloud climatology structure in time and space parallels the VOCAR soundings and is consistent with the concept that the marine-layer depth is related to the stratus cloud in the layer. Figure 14 is a proxy map of the relative marine-layer depth structure and its diurnal trend over the Southern California Bight. The result confirms that the lowest marine layer in the area is in the western mouth of the Santa Barbara channel and that there is a higher marine layer on the north side of the Pt. Arguello.

g. Along-coast, diurnal winds

Pressure differences between B54 and B53 are only modestly correlated with B53 winds (Fig. 15). But during some periods, the relationship is weak. The maximum, late afternoon, down channel pressure difference, which is the same for the 4th through the 10th of June 1996, is not correlated with the B54 wind speed maximum that ranges from 13 m s^{-1} on the 4th to 5 m s^{-1} on the 7th and then 15 m s^{-1} on the 10th. Figure 15 also illustrates the comparison between B54 and B53, with the former having periods with high westerly winds with lesser diurnal variation. Station B53 continues to have weak speeds at night, increasing to only about one-half to two-thirds of B54's speed during the afternoon.

All of the winds at stations on the narrow, north coastal plain (zone 3), with the exception of GAVW, have a striking diurnal, alongshore, reversing character. Closer examination was made for phase relationships between the coastal land stations. GAVE and WCAM both had reversing diurnal shifts in the wind on 87% of the summer days, which is typical of the other stations. For GAVE and EMMA, it was found that in the late morning, both stations reverse direction from easterly to westerly and increase in speed until near 1600 PST and EMMA's diurnal maximum. On the other hand, GAVE, some 219 km to the west of EMMA, reverses within an hour to a maximum in the opposite direction. Out of the summer, this near-instant reversing of GAVE while EMMA was still strong westerly occurred on 36% of the days. There was an approximately even amount of these where the reversal occurred simultaneous with EMMA's peak wind as opposed to a little latter while EMMA was still strong westerly.

The wind direction reversal from westerly to easterly in the afternoon/early evening clearly began at the westernmost station (GAVE) and ended with the easternmost station (EMMA) on 39% of the summer days. The approximate timing of these reversals was such that ECAP was an hour later, WCAM was 2 h later, and EMMA was 4 h later.

The wind direction reversal from easterly to westerly in the morning is more uniform in timing without a dominant and distinctive phase trend as in the afternoon. However, in the morning reversals, EMMA reversed to westerly first on 47% of the summer days.

A schematic model is presented that summarizes the dominant diurnal relationship of the north coastal stations (zone 3) winds and the air temperature inversion structure (Fig. 16). In addition, it is assumed that there

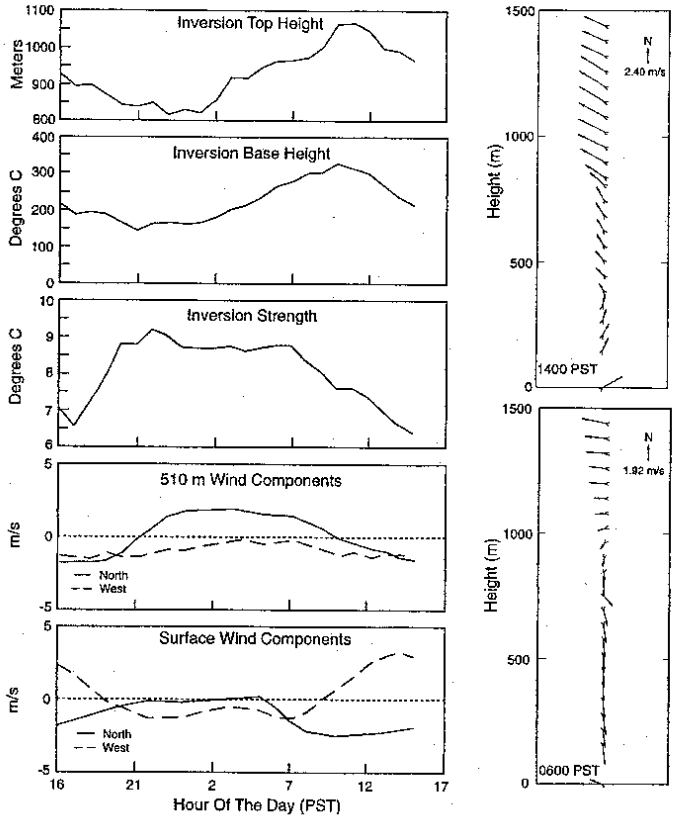

FIG. 11. Selected diurnal trends at the Goleta profiler (GOLE). The air temperature inversion base is a minimum at 2100 PST and a maximum at 1000 PST. Shown on the right is the mean profile for (upper) 1400 PST and (lower) 0600 PST.

is a density-driven, up–mountain slope flow that peaks in the afternoon and a much weaker, down–mountain slope flow that peaks around sunrise (Atkinson 1981), which is consistent with our field experience although not directly measured. At 2100 PST, the inversion is at a minimum elevation, the surface winds are westerly, and the inversion wind is weak. At 0000 PST, the inversion is rising and the inversion base winds are a maximum from the north. By 0600 PST, the inversion base has lifted to the halfway point while the weak downslope flow is a maximum. At 1000 PST, the inversion base is at its maximum elevation, the surface winds are weakly from the south and the inversion winds are weak. By 1400 PST, the inversion base is sinking, the surface winds are peaking in westerly speed while the inversion winds are from the south. Near this time, solar heating maximizes an upslope flow with a subsiding return flow in the inversion over the coast. At 1700 PST, the inversion base has settled to the halfway point and it reaches the minimum elevation at 2100 PST to complete the diurnal cycle.

The general picture is that the inversion base over the coast sinks and the surface winds are from the west during the afternoon. At night, the inversion base lifts and the surface winds are from the east. A cross-coast circulation is set up by the density-driven slope flow that is in the opposite direction of the inversion vertical motion. It is suggested that the inversion base height over the north side of the channel is being forced by the diurnal changes in the overwater expansion fan. This would explain the similar nature of the surface winds at JALM that is around the corner of Pt. Conception

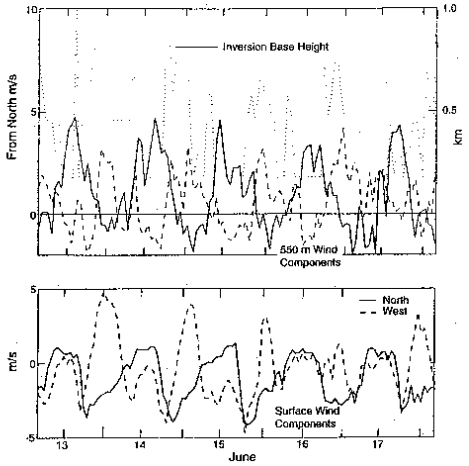

FIG. 12. A short time series showing phase relationship at the Goleta profiler (upper frame). At 550-m elevation, north wind component (solid) is at quadrature to the west component (dashed) in the diurnal period. The inversion base height (dotted) has a distinct, diurnal period too, with a maximum in the late morning, when the 550-m winds are reversing. Surface wind components at Goleta are in the lower frame.

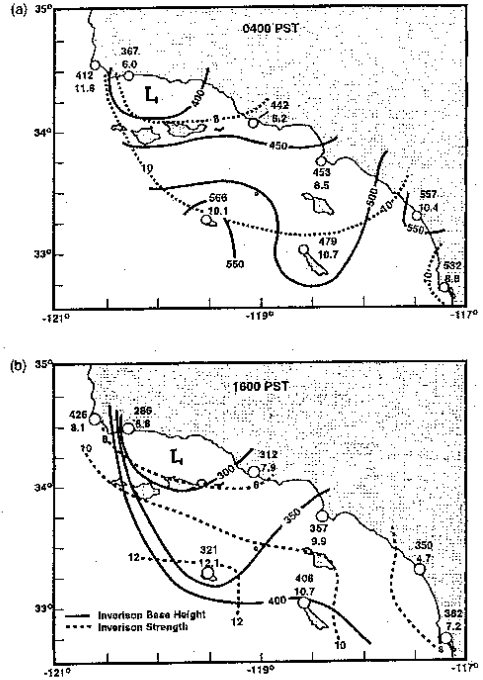

FIG. 13. (a) 0400 PST inversion base height (solid) and strength (dashed). Station's locations are at circles, where the upper plotted number is the air temperature inversion base height in meters and the lower number is the inversion strength in °C. (b) 1600 PST inversion base height and strength. The lowest inversion base height is over the Santa Barbara Channel at both times.

but tucked between the high speed, northerly wind stations of PARG and PCON. However, there is considerable day-to-day variability in the phase of the north coast station reversals.

5. Winter structure and variations

a. Mean fields

Mean winter winds are for the December 1995–February 1996 period for all stations except B11 and JALM. The December 1994–February 1995 observations are used to compute the mean for B11 and JALM as these stations were not available for the 1995/96 season. The winter wind mean and PA for the surface stations are from the northwest at the western mouth and turn to the east in the Santa Barbara Channel (Fig. 17) as during the summer. However, drainage resulting from colder night temperature over the elevated topography flows down the Ventura River valley and causes offshore wind at ERIO, EMMA, and GAIL. There is a mean offshore flow over the north coast stations in contrast to summer. Winter standard deviations are larger than the mean winds and also greater than the summer standard deviations.

Mean winter sea surface pressure gradients are weaker in the winter (Fig. 6). The winter cross-channel gradient is small. The lowest pressures are to the east, as in summer, but the along-channel gradient is half what it is in the summer. This suggests that the vertical thermal structure is uniform across the Santa Barbara Channel in the winter.

b. Correlations and EOFs

Correlations between the overwater wind component along the PA (Fig. 17) are greater in the winter than the summer, which may be due to the longer horizontal scale of winter synoptic events than the summer mesoscale structure. Most of the overwater stations have correlations of 0.7–0.8 or better with neighboring stations. The lowest correlation between a central channel station (B54) and a near-coast station (GAVE) dips to only 0.69. Even the stations away from the Santa Barbara Channel (B11, B25) are correlated with those in it. The poorest correlations are between the land stations at the eastern end of the Santa Barbara Channel.

Winter eigenvectors 1 and 2 are almost the same for the summer (Fig. 17), which confirms the dominant role the local topography plays in surface wind alignment. However, the distribution of eigenvectors (Table 3) is

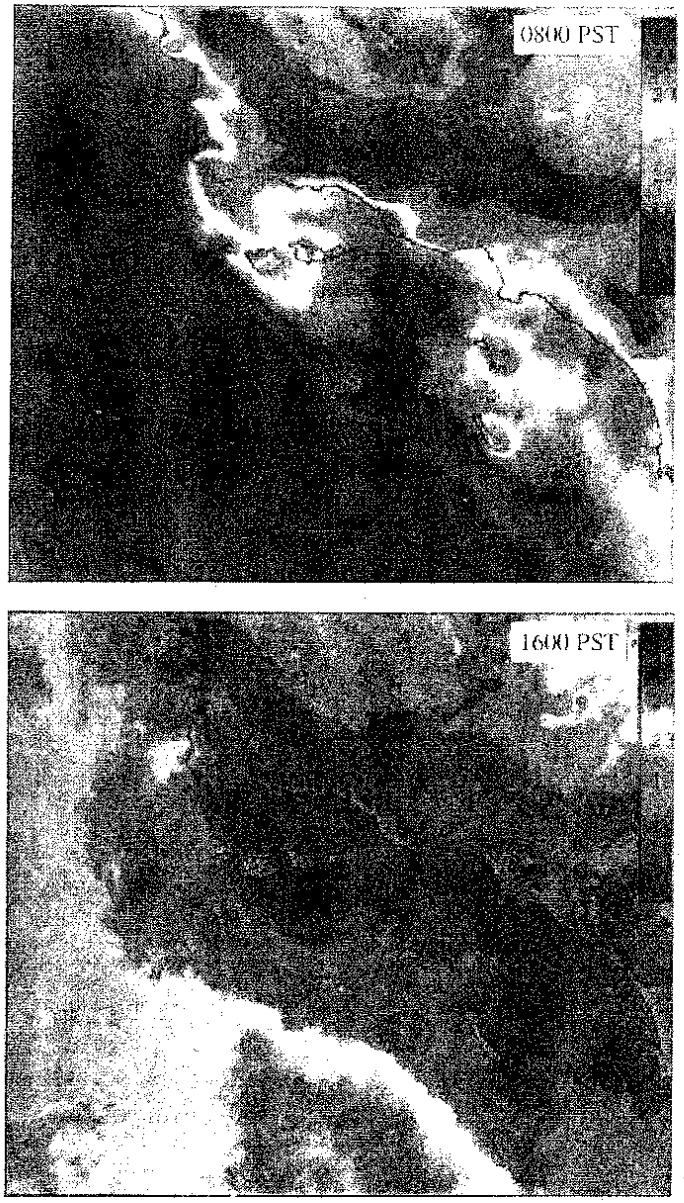

FIG. 14. Average *GOES-9* visual cloud image for 0800 PST (upper) and 1600 PST (lower). The albedo color scale is given in the upper right. The least cloud cover is in the western mouth of the Santa Barbara Channel. At 0800 PST, there is a relatively high cloud cover to the north of Pt. Conception where the marine layer has pushed up against and overrun higher topography. At 1600, clearing continues in the Santa Barbara Channel while the clouds have increased over the edge of land north of Pt. Conception.

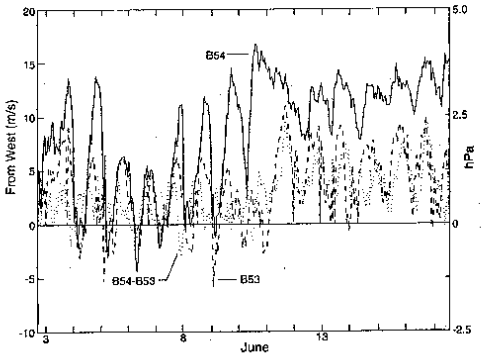

FIG. 15. Summer wind component along PA for B54 (solid) and B53 (dashed) and pressure difference for B54–B53 (dotted). This represents the situation along the central portion of the channel. The pressure difference along the center of the channel is often poorly related to the winds in the western portion and more closely related to those in the eastern portion.

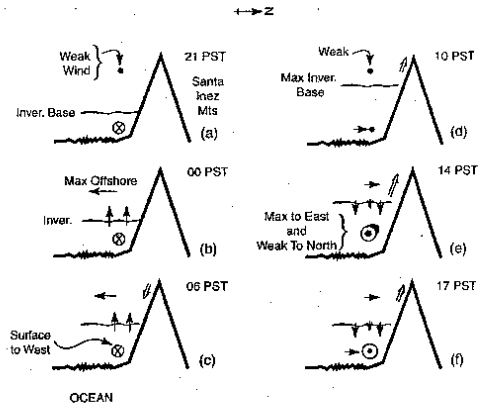

FIG. 16. Westward-looking schematic model of the relation between the north coast station winds and the inversion base height. Mountain up and downslope flow is represented by double arrows.

quite different, reflecting the larger correlation scales. More frequent synoptic-scale variations in the winter cause more persistent peaks in the time series of the winter eigenvector 1 than the summer (Fig. 7). The magnitude and variation of eigenvector 2, which is the diurnal scale, is the same in summer and winter.

c. *Synoptic variability*

A late-December 1995 case is typical of strong southerly sea level winds followed by a reversal to strong northerly winds. The synoptic situation for strong southerly winds is an approaching front off California and a deep low extending from sea level to above 500 hPa. Sea level and midlevel winds are from the south along central California and the western portion of the Southern California Bight. Later, by 28 December, a ridge oriented northeast–southwest developed across central California from sea level to above 500 hPa and a trough to the east of California. The result was strong winds from the northwest from sea level to the upper atmosphere over the Santa Barbara Channel.

Strong southerly winds at the western Santa Barbara Channel surface stations extended from 22 to 26 December with the winds increasing in strength from the Islands to B51 (Fig. 18). Winds were slower and from the east in the eastern portion of the channel. North coastal stations varied between periods of southerly and alongshore winds.

The winds reversed abruptly around midnight on 26–27 December to be strong from the north-northwest of the western channel until 1 January. Winds increased from B51 to maximum at B54 then mildly decreased at the islands. The north coast stations such as GAVE experienced persistent offshore winds but at speeds less than at the islands. Finally, winds were weak and variable in direction at the eastern coastal station ERIO.

d. *Diurnal variability*

Winter diurnal trends over the water (not shown) have a phase relation similar to diurnal trends during the summer. However, the diurnal range is less and the over-water stations' values are reduced at all hours. The exception is the Oxnard station at ERIO, which has a stronger and longer duration easterly component lasting from 1900 to 0900 during the winter.

Winter air temperatures shown in Fig. 19 are for the December 1995–February 1996 period for all stations except B11, PARG, and JALM, for which December 1994–February 1995 has been substituted. In the winter morning, there is a weak air temperature maximum over the center of the channel while the strongest minimum is over the Oxnard Plain on the eastern end. By the afternoon, stronger diurnal warming has reversed the situation so that the warmest temperatures are over land. Somewhat similar to the summer, there are along- and cross-channel gradients with the coldest air at the western mouth of the channel. However, satellite-derived SSTs (thin dashed lines in Fig. 19) are nearly uniform over the Santa Barbara Channel.

6. Eddies

Two eddies have been found in the sea level wind field over the Santa Barbara Channel based upon September–October 1980 observations collected for an air pollution study that are presented in Fig. 20 (Smith et al. 1983; Dabberdt and Viezee 1987; Douglas and Kessler 1991; Hanna et al. 1991). We find that these are typical of neither the summer nor the winter, although

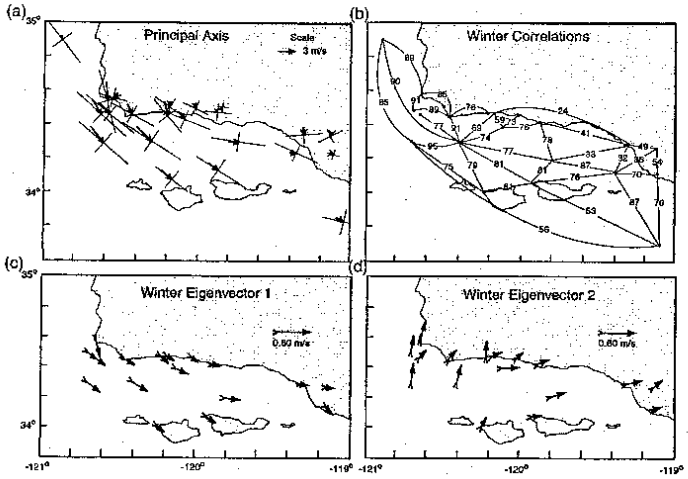

FIG. 17. (a) Winter mean surface wind speed and principle axis (PA). See Fig. 4 for explanation. (b) Winter wind correlations along station PAs. (c) and (d) First and second empirical orthogonal functions for the winter (lower panels).

this probably reflects the different time periods of the studies and the focusing on a particular light wind situation that is associated with late summer air pollution events.

The first is in regards to an evening, midchannel, cyclic eddy (Smith et al. 1983) (Fig. 20a). The midchannel buoys (B54, B53) and platform GAIL showed that the marine air moves zonally along the center of

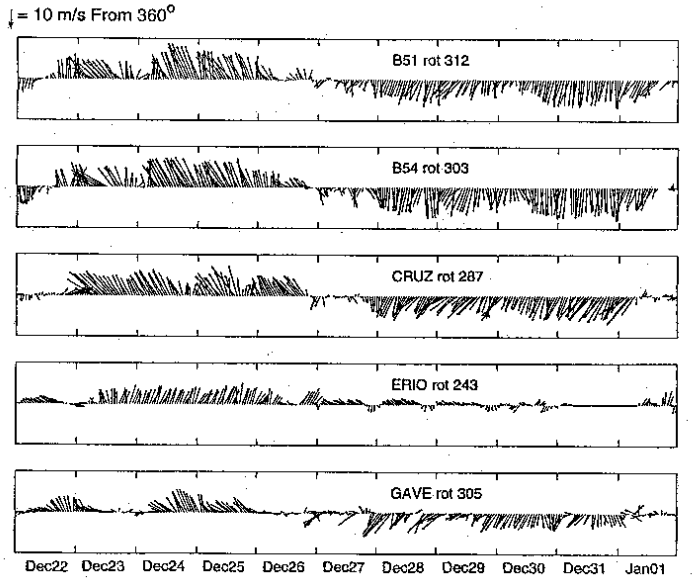

FIG. 18. Surface station wind vector series rotated to the PA for 22 Dec 1995–2 Jan 1996.

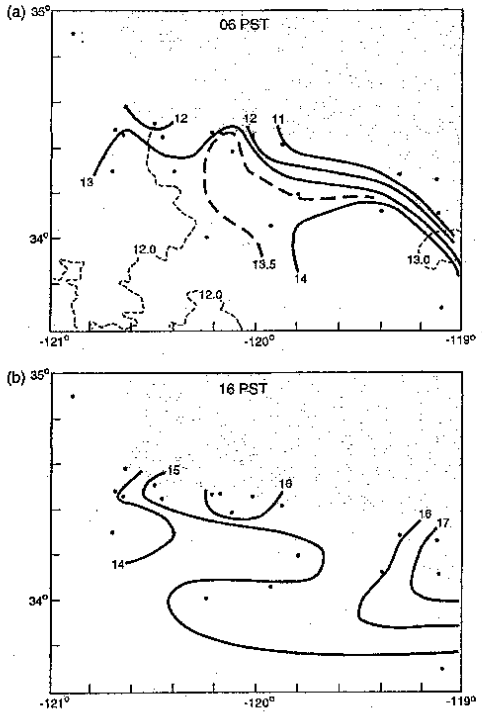

FIG. 19. Winter mean air temperatures (°C) at (a) 0600 PST and (b) 1400 PST. The winter SSTs estimated from satellite infrared images are superimposed on the upper chart as thin dashed lines.

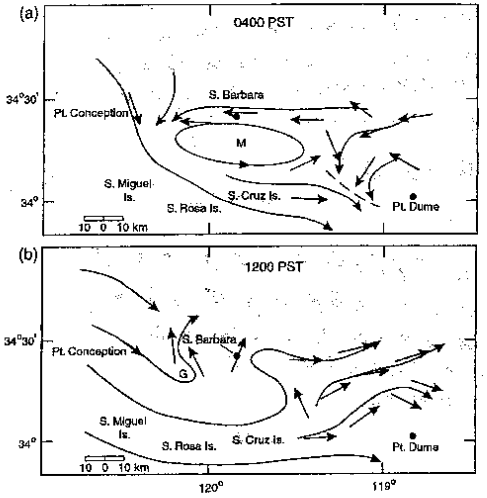

FIG. 20. Streamlines of most frequent September wind directions from Smith et al. (1983) and Dabberdt and Viezee (1987). Arrows are measured winds. Here M marks midchannel eddy in (a) and G denotes Gaviota eddy in (b).

the channel and from the west. The majority of this air mass moves from the northwest past GAIL, whereas the air pollution analysis had winds from the southeast at GAIL. Our analysis suggests that if the winds at B54 are strong, there is no midchannel eddy, which occurs most of the time.

In addition, our analysis does not support a summer, daytime Gaviota eddy in the lee of Pt. Conception (Fig. 20b), although this may be partly semantics. Our analysis suggests that the dominant winds between Gaviota (GAVE) to Ventura (EMMA) are coast-parallel and diurnally reversing. The along-coast afternoon winds are part of the zonal, westerly flow, unlike the cross-shore, coastal winds found during the air pollution studies. Easterly, evening winds over the coastal stations are consistent with the earlier studies, but there is a very narrow transition zone into the westerly and stronger flow over most of the channel. We would classify this as a shear zone, rather than an eddy owing to the difference in speeds and the narrowness of the transition between the two flow directions. We also find a different phase relationship among the coastal stations, such that the western coastal stations will reverse before the eastern coastal station (EMMA). On most of the days, especially under lighter winds, the finer aspects of the timing of the direction changes at the coastal stations are erratic, defying simple classification.

7. Dynamical interpretation

a. A model

The presence of a marine layer between the ocean and the free atmosphere with distinct air mass properties allows for the existence of gravity waves, which can propagate along the inversion. The existence of these waves has been documented in a number of studies (Atkinson 1981), and different models for the wave propagation have been proposed (Gossard and Hooke 1975). The possibility for gravity waves to exist and propagate at some speed also has implications for steady flows, and hydraulic flow theory provides the context for describing the development of such flow (Ippen 1951). The behavior of a steady hydraulic flow depends critically on the Froude number, the ratio of the flow speed, and the speed of gravity waves propagating on the inversion. If the Froude number is less than unity, the presence of obstacles in the flow can extend upstream of the obstacle and the flow is subcritical. If the Froude number is greater than one, no flow adjustment can occur upstream and the flow is supercritical (Samelson 1992).

Observations of the marine layer off the California

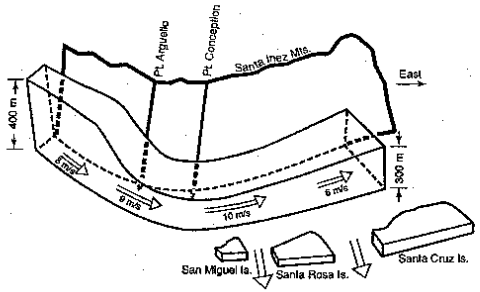

FIG. 21. Schematic model of the marine-layer structure turning into the Santa Barbara Channel. The marine air thins, expands, and accelerates as it turns the corner into the Santa Barbara Channel, causing the fastest winds to be at the western mouth.

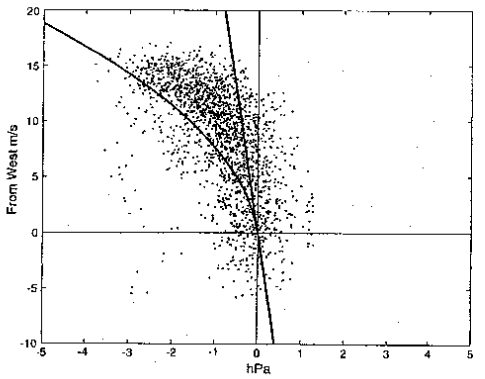

FIG. 22. Scatterplot of hourly B54 wind as a function of the HOND–ROSA pressure difference. The straight line is the expectation if there were a purely geostrophic balance. The quadratic line is the expectation if there were a strong supercritical expansion.

coast (Dorman 1985b; Winant et al. 1988; Samelson and Lentz 1994) suggest that at any time the flow can shift between sub- and supercritical conditions as a function of position, a condition described as transcritical (Rogerson 1999).

The conditions in the western mouth (zone 1) are very much like a supercritical or transcritical expansion fan in the lee of a corner. A schematic model in Fig. 21 summarizes the details. Under strong, supercritical flow to the south or southeast, the near–sea level air accelerates from around the area between Pt. Arguello and Pt. Conception to the speed maximum, near B54. At the same time, the atmospheric marine layer expands and thins to a minimum height and the sea level pressure decreases. The inversion also tilts downward to the north across the channel, making the lowest inversion base along the north coast as shown in Fig. 13. As marine air continues eastward toward B53, it slows and the vertical dimension increases. Some of the air mass entering the western mouth exits at supercritical speeds via the gaps between the channel islands. The low air temperature inversion base over the north coast intersects the topography, capping the marine air and limits vertical exchange. With no outlet to the north, the coastal winds run parallel to the coast, even during the height of diurnal heating cycle.

The descriptive details provided in the preceding sections support this model. The surface winds accelerate into the mouth to a maximum speed, then decrease toward the eastern portion of the channel. Fixed soundings show that the Santa Barbara Channel has the lowest inversion base in the Southern California Bight. Satellite cloud averages have structures that are consistent with deeper marine layers outside the western mouth, lowering into the western Santa Barbara Channel. Cloud analysis also confirms lower clouds and supercritical expansion in the lee of the gaps between the Channel Islands.

The lack of sounding data over water and north of Pt. Conception prevents a clear identification as to the Froude number of the inbound marine layer. However, the relatively low velocities and deeper marine layer at B11 suggests that both the inbound flow and the outbound velocities in the eastern half of the Santa Barbara Channel are subcritical. Only the western mouth of the channel is supercritical. This pattern conforms to the transcritical flow in the lee as described by Rogerson (1999).

b. Supercritical flow and surface stations

Whether or not the Froude number is greater than one and the flow is supercritical can be estimated from the sea level wind and pressure observations at the western mouth. The cross-channel pressure gradient can be computed from SROS minus HOND pressures, which are separated by 40 km. The along-PA component at B54 was used for the surface wind. A scatterplot of the pressure difference versus wind speed for May–July 1996 is presented in Fig. 22. If the momentum balance is geostrophic, the pressure difference may be related to the wind speed by the following geostrophic relationship,

$$dP = \rho f V\, dx,$$

where ρ is the density, f is the Coriolis parameter, V is the wind speed perpendicular to the two stations, and dx is the pressure station separation. As noted in Winant et al. (1988), using a modification of Bernoulli's equation we can compute the maximum pressure difference expected if the flow is supercritical and frictionless, and if the inbound Froude number is one and the downstream Froude number is infinite. Across the expansion fan, the speed should be related to the pressure by the quadratic,

$$dP = \rho V(f\, dx - V),$$

which represents the sum of the geostrophic difference and the maximum difference expected for a supercritical expansion. The density is assumed to be 1.2 kg m^{-3}, the Coriolis parameter is 8.2×10^{-5} s^{-1}, and the distance between the pressure stations is 40 km. Most of the intermediate and higher speeds fit between the quadratic and the line that is also plotted in Fig. 22. A similar result was found in the lee of Pt. Arena by Winant et al. (1988) and supports the existence of a transcritical expansion fan.

c. Summer versus winter

It is useful to compare the summer and winter seasons for the role of supercritical flow in modifying characteristics. The summer sea level pressure gradient is both stronger and asymmetrical across the channel (lower on the north side). A major contributor to the asymmetry is the thinner marine layer on the north side. For every 100 m below the marine layer, the surface pressure would be reduced by the order of 0.5 hPa (Dorman 1985a). That the marine layer is low in the Santa Barbara Channel is confirmed by the VOCAR and other limited sounding programs and supported by the satellite cloud climatology.

Summer sea level air temperatures are a minimum in the western mouth of the Santa Barbara Channel and are not apparent in the winter mornings. The difference is the summer's stronger westerly winds in the western mouth force upwelling and attendant SST minimums with a similar pattern. In the winter, the SST gradient is almost flat.

Summer mean winds over the western mouth of the Santa Barbara channel are faster than in the winter, although the standard deviation of the winds is similar in both seasons. Winter experiences strong winds either from a northerly or a southerly direction. On the other hand, only summer experiences strong winds from a northerly direction. They are also weak in the easternmost part of the channel, offshore from the Oxnard plain. Air temperature at the surface follows the SST closely and varies significantly with location. Sea level pressure gradients are correspondingly large. The height of the marine layer varies generally between 300 m in the late afternoon and 350 m in the late morning.

In winter, synoptic conditions are driven by traveling cyclones, sometimes accompanied by fronts. These are usually preceded by strong southeast winds and followed by strong northwest winds. Atmospheric parameters are distributed more uniformly than in summer and diurnal variations are greatly reduced. Sea level air temperature and pressure are more uniform spatially than in the summer.

Spatial variations in the observed fields in the summer are consistent with a hydraulic model of the MABL involving a transcritical expansion fan. The summertime situation is governed by a coupled interaction between the atmosphere and the underlying water. The ocean influences the density of the MABL to the extent that it behaves distinctly from the free atmosphere above, resulting in strong winds polarized in the direction parallel to the coast. In turn these winds provoke an upwelling response in the coastal ocean, which in part determines the surface properties of the water as is noted in Harms and Winant (1998).

8. Conclusions

Weather patterns in the Santa Barbara Channel vary markedly depending on the season. In late spring, summer, and fall, the weather results from the interaction between two persistent large-scale systems, the North Pacific anticyclone and the thermal low located over the southwestern United States. Partly because of the subsidence associated with the anticyclone, a well-defined marine atmospheric boundary layer (MABL) with properties distinct from the free atmosphere above is a conspicuous feature during the summer. The wind has different characteristics in each of three zones. Maximum winds occur in the area extending south and east from Pt. Conception, where they initially increase as they turn to follow the coast, then decrease farther east. Winds are generally weaker, sometimes reversing to easterly at night, in a narrow band along the mainland coast.

Acknowledgments. We are especially grateful to the Santa Barbara Air Pollution Control District, the Ventura Air Pollution Control District, and Point Mugu NAS for sharing data that was essential for this analysis. Lee Eddington supplied data from the navy-sponsored VOCAR program. Dick Lind was crucial in capturing and transferring upper-air data. David Browne of MMS helped obtain access to platforms and was an essential link to the core funding. This paper was funded by the Mineral Management Service and the Office of Naval Research.

REFERENCES

Atkinson, B. W., 1981: *Meso-Scale Atmospheric Circulations.* Academic Press, 495 pp.

Baynton, H. W., J. M. Bidwell, and D. W. Beran, 1965: The association of the low-level inversions with surface wind and temperature at Point Arguello. *J. Appl. Meteor.*, **4,** 509–516.

Bosart, L. F., 1983: Analysis of a California Catalina eddy event. *Mon. Wea. Rev.*, **111,** 1619–1633.

Brink, K. H., and R. D. Muench, 1986: Circulation in the Point Conception–Santa Barbara Channel region. *J. Geophys. Res.*, **91,** 877–895.

Caldwell, P. C., D. W. Suart, and K. H. Brink, 1986: Mesoscale wind variability near Point Conception, California, during spring 1983. *J. Climate Appl. Meteor.*, **25,** 1241–1254.

Clark, J. H. E., and S. R. Dembek, 1991: The Catalina eddy event of July 1987: A coastally trapped mesoscale response to synoptic forcing. *Mon. Wea. Rev.*, **119,** 1714–1735.

Dabberdt, W. F., and W. Viezee, 1987: South Central Coast Cooperative Aerometric Monitoring Program (SCCCAMP). *Bull. Amer. Meteor. Soc.*, **68,** 1098–1110.

Dana, R. H., 1841: *Two Years Before the Mast: A Personal Narrative of Life at Sea.* Harper, 483 pp.

DeMarrias, G. A., G. C. Holzworth, and C. R. Hosler, 1965: Meteorological summaries pertinent of atmospheric transport and dispersion over southern California. U.S. Weather Bureau Tech. Paper 54, 86 pp. [Available from Superintendent of Documents, U.S. Government Printing Office, Washington, DC 20401.]

Dorman, C. E., 1982: Winds between San Diego and San Clemente Island. *J. Geophys. Res.*, **87**, 936–946.

——, 1985a: Evidence of Kelvin waves in California's marine layer and related eddy generation. *Mon. Wea. Rev.*, **113**, 827–839.

——, 1985b: Hydraulic control of the northern California marine layer. *Eos, Trans. Amer. Geophys. Union*, **66**, 914.

——, 1987: Possible role of gravity currents in northern California's coastal summer wind reversals. *J. Geophys. Res.*, **92**, 1497–1506.

——, and C. D. Winant, 1995: Buoy observations of the atmosphere along the west coast of the United States, 1981–1990. *J. Geophys. Res.*, **100**, 16 029–16 044.

Douglas, S. G., and R. C Kessler, 1991: Analysis of mesoscale airflow patterns in the south-central coast air basin during the SCCCAMP 1985 intensive measurement periods. *J. Appl. Meteor.*, **30**, 607–631.

Eddington, L. W., 1985: A numerical simulation of a topographically forced wind maximum in a well-mixed marine layer. OPUS Tech. Rep. 16, FSU-MET-OPUS-85-1, 61 pp. [Available from Dept. of Meteorology, The Florida State University, Tallahassee, FL 32306.]

——, J. J. O'Brien, and D. W. Stuart, 1992: Numberical simulation of topographically forced mesoscale variability in a well-mixed marine layer. *Mon. Wea. Rev.*, **120**, 2881–2896.

Edinger, J. G., 1959: Changes in the depth of the marine layer over the Los Angeles basin. *J. Atmos. Sci.*, **16**, 219–226.

——, 1963: Modification of the marine layer over coastal southern California. *J. Appl. Meteor.*, **2**, 706–712.

——, and M. G. Wurtele, 1972: Interpretation of some phenomena observed in southern California stratus. *Mon. Wea. Rev.*, **100**, 389–398.

Fisk, C., 1994: Mesoscale hourly variation in surface meteorological parameters during the intensive operation of Vocar 22 August 1993–4 September 1993. Geophysics Division Tech. Note No. 187, 43 pp. [Available from Naval Air Warfare Center, Weapons Division, Point Mugu, CA 93042-5001.]

Gossard, E. E., and W. H. Hooke, 1975: *Waves in the Atmosphere, Atmospheric Infrasound and Gravity Waves—Their Generation and Propagation.* Elsevier, 456 pp.

Halliwell, G. R., and J. S. Allen, 1987: The large-scale coastal wind field along the west coast of North America. *J. Geophys. Res.*, **92**, 1497–1506.

Hamilton, G. D., 1980: NOAA Data Buoy Office programs. *Bull. Amer. Meteor. Soc.*, **61**, 1012–1017.

Hanna, S. R., D. G Strimaitus, J. S. Scire, G. E. Moore, and R. C. Kessler, 1991: Overview of results of analysis of data from the South-Central Coast Cooperative Aerometric Monitoring Program (SCCCAMP 1985). *J. Appl. Meteor.*, **30**, 511–533.

Harms, S., and C. D. Winant, 1998: Characteristic patterns of the circulation in the Santa Barbara Channel. *J. Geophys. Res.*, **103**, 3041–3065.

Ippen, A. T., 1951: Mechanics of supercritical flow. *Trans. Amer. Soc. Civ. Eng.*, **116**, 268–295.

Kessler, R. C., and S. G. Douglas, 1991: Numerical study of mesoscale eddy development over the Santa Barbara Channel. *J. Appl. Meteor.*, **30**, 633–651.

Large, W. G., and S. Pond, 1981: Open ocean momentum flux measurements in moderate to strong winds. *J. Phys. Oceanogr.*, **11**, 324–481.

Lorenz, E. N., 1956: Empirical orthogonal functions and statistical weather prediction. MIT Sci. Rep. 1, 49 pp. [Available from Stat. Forecasting Project, Department of Meteorology, Massachusetts Institute of Technology, Cambridge, MA 02139.]

Mass, C. F., and M. D. Albright, 1987: Coastal southerlies and alongshore surges of the west coast of North America: Evidence of mesoscale topographically trapped response to synoptic forcing. *Mon. Wea. Rev.*, **115**, 1707–1738.

——, and ——, 1989: Origin of the Catalina eddy. *Mon. Wea. Rev.*, **117**, 2406–2436.

Neiburger, M., D. S. Johnson, and C. W. Chien, 1961: Studies of the structure of the atmosphere over the eastern Pacific Ocean in the summer. *The Inversion over the Eastern North Pacific Ocean*, University of California Press, 1–94.

Nelson, C. S., 1977: Wind stress and wind stress curl over the California Current. NOAA Tech. Rep. NMFS SSRF-714, 87 pp. [Available from National Oceanic and Atmospheric Administration, Monterey, CA 93940.]

——, and D. M. Husby, 1983: Climatology of surface heat fluxes over the California current region. NOAA Tech. Rep. NMFS SSRF-763, 155 pp.

Paulus, R. A., 1995: An overview of an intensive observational period on variability of coastal atmospheric refractivity. *Proc. AGARD/NATO Conf. on Propagation Assessment in Coastal Environments*, Bremerhaven, Germany, NATO, 1–6.

Ralph, F. M., L. Armi, J. M. Bane, C. E. Dorman, W. D. Neff, P. J. Neiman, W. Nuss, and P. O. G. Persson, 1998: Observations and analysis of the 10–11 June 1994 coastally trapped disturbance. *Mon. Wea. Rev.*, **126**, 2435–2465.

Reason, C. J. C., and D. G. Steyn, 1992: The dynamics of coastally trapped mesoscale ridges in the lower atmosphere. *J. Atmos. Sci.*, **49**, 1677–1692.

Rogerson, A. M., 1999: Transcritical flows in the coastal marine atmospheric boundary layer. *J. Atmos. Sci.*, **56**, 2761–2779.

Rosenthal, J., 1968: A Catalina eddy. *Mon. Wea. Rev.*, **96**, 742–743.

——, 1972: Point Mugu Forecasters Handbook. Pacific Missile Range, Tech. Publ. PMR-TP-72-1, 324 pp. [Available from Geophysics Branch, Pacific Missile Range, Pt. Mugu, CA 93042-5001.]

Ryan, G., 1996: Downslope winds of Santa Barbara, California. NOAA Tech. Memo. NWS WR-240, 44 pp. [Available from National Technical Information Service, U.S. Department of Commerce, 5285 Port Royal Rd., Springfield, VA 22161.]

Samelson, R. M., 1992: Supercritical marine-layer flow along an smoothly varying coastline. *J. Atmos. Sci.*, **49**, 1571–1584.

——, and S. J. Lentz, 1994: The horizontal momentum balance in the marine atmospheric boundary layer during CODE-2. *J. Atmos. Sci.*, **51**, 3745–3757.

Smith, T. B., W. D. Saunders, and F. H. Shair, 1983: Analysis of Santa Barbara oxidant study. Final Report to California Air Resources Board, Agreement A2-086-32, 236 pp. [Available from Meteorology Research, Inc., Altadena, CA 91001.]

Sommers, W. T., 1978: LFM forecast variables related to Santa Ana wind occurrences. *Mon. Wea. Rev.*, **106**, 1307–1316.

Thornthwaite, C. W., W. J. Superior, and R. T. Field, 1965: Disturbance of airflow around Argus Island Tower near Bermuda. *J. Geophys. Res.*, **70**, 6047–6052.

Wakimoto, R. M., 1987: The Catalina eddy and its effects on pollution over southern California. *Mon. Wea. Rev.*, **115**, 837–855.

Winant, C. D., C. E. Dorman, C. A. Friehe, and R. C. Beardsley, 1988: The marine layer off northern California: An example of supercritical channel flow. *J. Atmos. Sci.*, **45**, 3588–3605..